Stem Cell Reports
Article

ISSCR

OPEN ACCESS

Mesenchymal to Epithelial Transition Mediated by CDH1 Promotes Spontaneous Reprogramming of Male Germline Stem Cells to Pluripotency

Junhui An,[1] Yu Zheng,[1] and Christina Tenenhaus Dann[1,*]
[1]Department of Chemistry, Indiana University, Chemistry A025, 800 E. Kirkwood Avenue, Bloomington, IN 47405-7102, USA
*Correspondence: ctdann@indiana.edu
http://dx.doi.org/10.1016/j.stemcr.2016.12.006

SUMMARY

Cultured spermatogonial stem cells (GSCs) can spontaneously form pluripotent cells in certain culture conditions. However, GSC reprogramming is a rare event that is largely unexplained. We show GSCs have high expression of mesenchymal to epithelial transition (MET) suppressors resulting in a developmental barrier inhibiting GSC reprogramming. Either increasing OCT4 or repressing transforming growth factor β (TGF-β) signaling promotes GSC reprogramming by upregulating CDH1 and boosting MET. Reducing ZEB1 also enhances GSC reprogramming through its direct effect on CDH1. RNA sequencing shows that rare GSCs, identified as CDH1$^+$ after trypsin digestion, are epithelial-like cells. CDH1$^+$ GSCs exhibit enhanced reprogramming and become more prevalent during the course of reprogramming. Our results provide a mechanistic explanation for the spontaneous emergence of pluripotent cells from GSC cultures; namely, rare GSCs upregulate CDH1 and initiate MET, processes normally kept in check by ZEB1 and TGF-β signaling, thereby ensuring germ cells are protected from aberrant acquisition of pluripotency.

INTRODUCTION

A long-standing vision for regenerative medicine has been the possibility of generating cells needed for therapy by inducing differentiation of pluripotent cells. Pluripotent cells are defined by their ability to give rise to all of the cell types that make up the body. Embryonic stem cells (ESCs) are the prototypical pluripotent cell type, derived from the inner cell mass within blastocyst staged embryos. Primordial germ cells (PGCs) can first be detected in the extraembryonic mesoderm just posterior to the definitive primitive streak in mouse at 7 days post coitum (dpc) (Ginsburg et al., 1990). In 1992, it was found that PGCs could reprogram into ESC-like (ESL) cells when cultured with appropriate growth factors including fibroblast growth factor 2 (FGF2), stem cell factor, and leukemia inhibitory factor (LIF) (Matsui et al., 1992; Resnick et al., 1992). The reprogramming potential of PGCs decreases gradually during development between 8.5 and 12.5 dpc, and reprogramming ability is no longer found in the embryonic germline later than 12.5 dpc (Labosky et al., 1994). However, the reprogramming ability is restored in later germline development as evidenced by the ability to derive ESL cells from spermatogonial stem cells (SSCs) (Guan et al., 2006; Kanatsu-Shinohara et al., 2004; Ko et al., 2009; Seandel et al., 2007).

SSCs are the founder cells of spermatogenesis and are located on the basement membrane of the seminiferous tubules. SSCs are unipotent and have the ability to self-renew to maintain a stem cell population or to differentiate to ultimately produce sperm. In 2003, an in vitro mouse SSC culture system was developed (Kanatsu-Shinohara et al., 2003). The cultured SSCs, designated germline stem cells (GSCs), form grape-like clusters in vitro and proliferate in medium containing several cytokines, notably glial cell line-derived neurotrophic factor (GDNF) (Kubota et al., 2004). Importantly, GSCs reinitiate spermatogenesis and produce offspring after transplantation into seminiferous tubules of infertile testes (Kanatsu-Shinohara et al., 2003; Kubota et al., 2004). When GSCs are subjected to suitable in vitro conditions they can spontaneously dedifferentiate into ESL cells without introducing any exogenous factors (see Table S1 for summary; Guan et al., 2006; Kanatsu-Shinohara et al., 2004; Ko et al., 2009; Seandel et al., 2007). ESL cells derived from GSCs are able to contribute to chimera formation, fulfilling this requirement for a bona fide pluripotent cell type (Guan et al., 2006; Ko et al., 2009). ESL cells have been shown to be more similar to ESCs than induced pluripotent stem cells (iPSCs) of somatic origin in terms of gene expression profiles, indicating that ESL cells might be better than iPSCs for therapeutic purposes (Ko et al., 2009). SSC reprogramming as a transcription factor-free reprogramming strategy could be greatly beneficial for clinical applications and could also be a powerful tool for studying the origin of totipotency during development.

Early SSC reprogramming studies relied on visual detection of unpredictable, very rare conversion events wherein a singular, smooth-edged and flattened ESC-like colony would be found and manually removed from the surrounding typical grape-like clusters of GSCs. The first report of such an occurrence was in 2004 by the Shinohara group, who obtained ESL cells from neonatal mouse testis with extremely low frequency (1 in 10^7 cells). Seandel et al. (2007) used a similar protocol for reprogramming, except that they started with GPR125$^+$ GSCs derived from adult

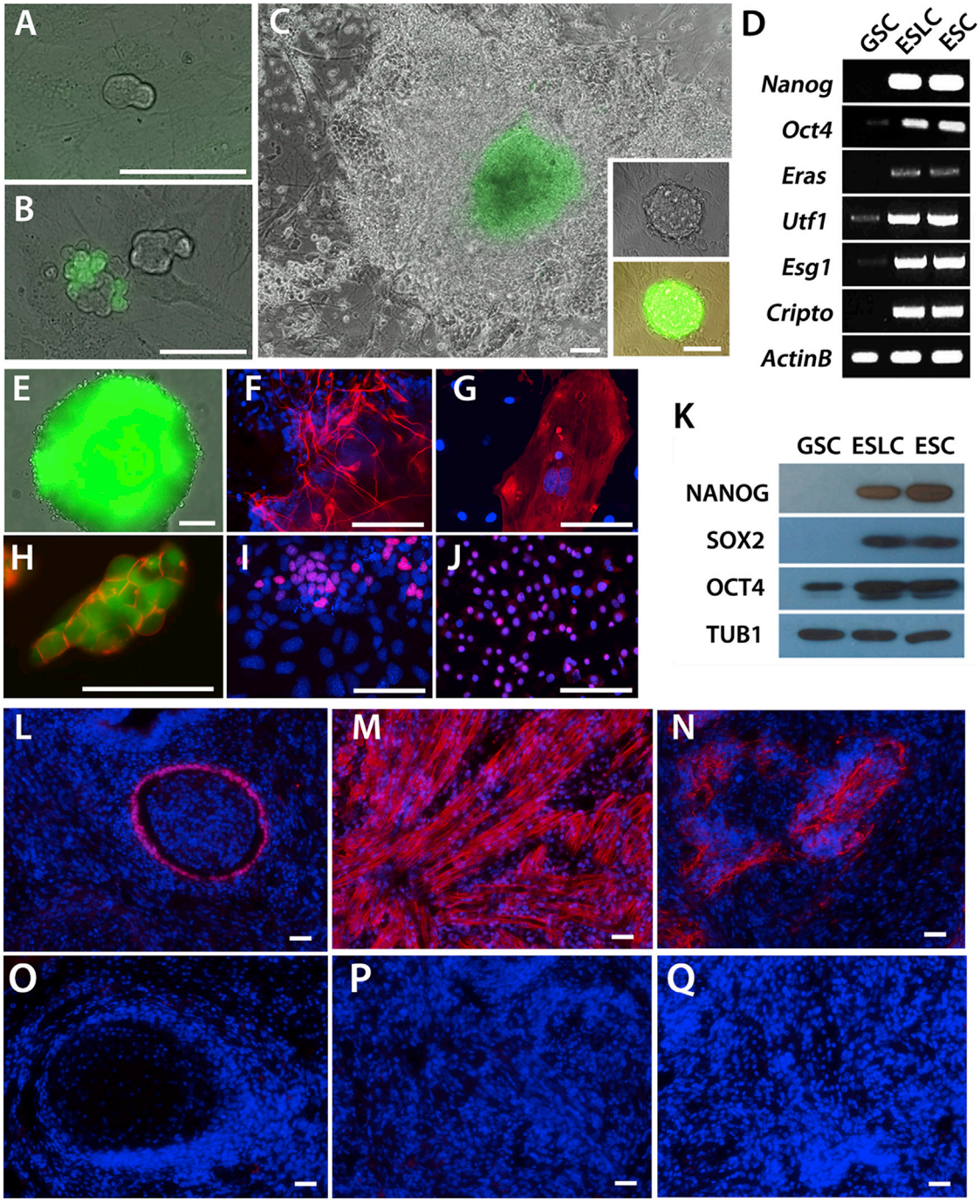

Figure 1. GSC Spontaneous Reprogramming and Characterization of ESL Cells

(A–C) Oct4-GFP GSC colony after (A) 3 days, (B) 14 days, or (C) 35 days of culture in RP medium. Insets show Oct4-GFP ESL cells derived from GSC colonies 7 days after transferring from GSC growth medium to ES medium. Scale bars, 150 μm.

(D) RT-PCR analysis of *Nanog*, *Oct4*, *Eras*, *Utf1*, *Esg1*, *Cripto*, and *ActinB* mRNA from GSC, ESL cells, and ES-D3 cells.

(E) Embryoid body derived from ESL cells. Green color indicates Oct4-GFP expression in (A) to (C), (E) and (H). Scale bar, 150 μm.

(F, G, I, and J) βIII-Tubulin immunostaining of neuron-like (ectodermal) cells derived by ESL cell differentiation (F). Immunofluorescence analysis of ESL-derived embryoid bodies differentiated into mesodermal cells (G, ACTA2), ectodermal cells (I, SOX1) and endodermal cells (J, GATA4) in red, merged with DAPI in blue.

(H) SSEA1 staining (red) in ESL cells.

(legend continued on next page)

mice and they used inactivated testicular stromal cells as a feeder layer. In contrast to the preceding reports, Ko et al. (2010) established a reprogramming protocol that converted GSCs, derived from adult Oct4-GFP mice, into ESL cells in a more predictable and reproducible manner. A key feature of their approach was that they determined an ideal density to plate cells for reprogramming that was 5- to 10-times lower than the typical density used for maintenance of GSCs, thereby allowing the cells to be cultured for 3–4 weeks without the need for dissociation and passaging.

GSC reprogramming takes place over multiple weeks and the mechanism is largely unknown. Low efficiency and inconsistent ESL cell formation makes it difficult to study the molecular mechanism of GSC reprogramming, knowledge of which is a prerequisite for improving the efficiency. In addition, GSCs do not reprogram to ESL cells when transfected with the four Yamanaka factors typically used in somatic cell reprogramming, suggesting that GSCs exhibit unique properties constituting a barrier to reprogramming (Morimoto et al., 2012). Here, we report that high TGF-β signaling and high ZEB1 expression result in a barrier preventing the needed upregulation of CDH1 for initiation of mesenchymal to epithelial transition (MET) during GSC reprogramming. Epithelial to mesenchymal transition (EMT) and the reverse process of MET are developmental processes whereby polar epithelial cells that typically interact with a basal membrane interconvert to fibroblast-like migratory cells with mesenchymal secretory properties. SSCs are generally not thought of as being either mesenchymal or epithelial but have certain properties of both epithelial cells (CDH1 expression) (Tokuda et al., 2007) and mesenchymal cells (THY1 expression) (Kubota et al., 2003).

In GSC clusters in vitro, and in undifferentiated spermatogonia in vivo, CDH1 is detected in a majority of cells (Fanslow et al., 2014; Tokuda et al., 2007). However, following dissociation of GSC clusters detection of CDH1 by flow cytometry varies depending on the exact method used. CDH1 epitopes are typically sensitive to trypsin digestion, a method commonly used for cell dissociation. We identified a population of rare CDH1$^+$ cells that remain following trypsin digestion (hereafter referred to simply as CDH1$^+$ GSCs). By total RNA sequencing (RNA-seq) analysis of trypsin-digested GSCs we show that CDH1- cells are mesenchymal-like and CDH1$^+$ GSCs are epithelial-like. The presence of a rare population of GSCs with epithelial properties, typified by enhanced CDH1 expression, likely explains the occasional spontaneous emergence of ESL cells that have been observed by others in standard GSC culture conditions in the past.

By focusing our study on understanding the molecular mechanism of GSC reprogramming we identify several key positive and negative regulators of the process and define manipulations that increase the CDH1$^+$ GSC population and promote MET and likewise, formation of ESL cells. First, we show CDH1 is essential for GSC reprogramming. Increasing OCT4 promotes reprogramming by upregulating CDH1 and boosting MET. ZEB1 and TGF-β signaling reduce CDH1 and suppress MET and GSC reprogramming efficiency. During the weeks-long process of reprogramming, CDH1$^+$ GSCs gradually increase and the enhanced reprogramming ability of isolated CDH1$^+$ cells suggests that CDH1$^+$ GSCs are poised in a later stage of MET. In summary, our results suggest that CDH1 upregulation constitutes a MET barrier to SSC spontaneous reprogramming that is controlled by ZEB1 and TGF-β signaling, thereby ensuring germ cells are protected from aberrant acquisition of pluripotency. Instead of relying on transfection of genetic material, we define multiple approaches that lead to improved conversion of mouse GSCs to pluripotency that may accelerate the study of human SSC reprogramming and its clinical applications.

RESULTS

Establishment and Validation of Conditions for Reproducible and Quantifiable GSC Reprogramming

In order to investigate mechanisms of GSC reprogramming we required a quantitative and reproducible assay (Figure S1). In a procedure adapted from Ko et al. (2010), Oct4-GFP GSCs were seeded at low density (Figure 1A) in wells of a 48-well plate and cultured in reprogramming medium (RP medium) without passaging for several weeks. Two weeks after plating, clusters were small (about 5–20 cells) and appeared similar to typical GSC clusters (Figure 1B). At this stage Oct4-GFP expression was heterogeneous and at overall low levels, consistent with what is known about OCT4 expression in GSCs (Dann et al., 2008) (Figure 1B). After 4 weeks GSC clusters often had more than 100 cells; abundant cell death was also observed, consistent with previous findings (Heim et al., 2012). However, in a subset of wells (~4 out of 100 wells; Table 1) a single colony emerged with typical ESC morphology and

(K) NANOG, SOX2, OCT4, and TUB1 immunoblotting of lysates from GSC, ESL, and ES-D3 cells.
(L–Q) Immunofluorescence analysis of ESL-derived teratomas differentiated into endodermal cells (L, GATA4), mesodermal cells (M, ACTA2), and ectodermal cells (N, βIII-tubulin) in red, merged with DAPI in blue. Respective negtive control images shown in (O–Q). Scale bars, 150 μm (E–J and L–Q).

Table 1. Summary of GSC/SSC Reprogramming Results

	Reprogramming Condition	Cell Background[a]	No. of Experiments	No. of Wells Cultured	No. of Wells with ESL Cells	ESL Colonies per 100 Wells
GSCs	RP medium only	OG/DO	5	96	4	4
		WT	2	96	3	
	+DMSO control	OG/DO	4	96	3	3
		WT	2	48	1	
	+siRNA control	OG/DO	6	96	3	3
		WT	3	72	2	
	+Dox	OG/DO	6	96	14	14
	+RepSox	OG/DO	5	96	13	12
		WT	2	48	4	
	+SB431542	OG/DO	4	84	3	4
	+*Zeb1* siRNA	OG/DO	6	120	17	13
		WT	3	72	8	
	+*Zeb2* siRNA	OG/DO	5	84	3	4
	+*Twist2* siRNA	OG/DO	5	84	2	2
	+*Zeb1* siRNA +control siRNA	OG/DO	4	96	12	10
		WT	3	72	5	
	+*Zeb1* siRNA +*Cdh1* siRNA	OG/DO	4	96	0	0
		WT	3	72	0	
	+Dox +*Cdh1* siRNA	OG/DO	2	96	0	1
		OG/DO	2	96	1	
	RP medium only	OG/DO $CDH1^+/THY1^+$	3	88	6	7
		OG/DO $CDH1^-/THY1^+$	3	96	1	1
Primary testis SSCs	+*Zeb1* siRNA	OG	3	72	5	7
	+siRNA control	OG	3	72	1	1
	+RepSox	OG	3	72	4	6
	+DMSO control	OG	3	72	2	3
	RP medium only	OG $CDH1^+/THY1^+$	4	84	5	6
		OG $CDH1^-/THY1^+$	4	84	0	0

[a]OG/DO, Oct4-GFP/Dox-Oct4; OG, Oct4-GFP; WT, wild-type.

unusually high GFP expression in the middle (Figure 1C). Upon trypsinization and transfer of all of the cells of each well to new wells containing standard ESC growth medium (ES medium), which contained LIF but lacked GDNF, the germ cells quickly died without GDNF but ESL cells formed typical ESC colonies and expanded rapidly within 1 week (Figure 1C). For quantitative assessment of reprogramming, reprogramming was defined by this ability of a well

of cells to rapidly expand upon dissociation and transfer to a new well containing ES medium.

To test whether the ESL cells had the same molecular phenotype as ESCs, we examined expression of pluripotency markers (Figures 1D and 1K). ESL cells expressed *Nanog*, *Oct4*, *Eras*, *Utf1*, *Esg1*, and *Cripto* mRNAs and stained positive for SSEA1, SOX2, and NANOG, but were negative for the SSC marker GFRA1 (Figures 1D, 1H, and S1). Western blotting confirmed NANOG, SOX2, and OCT4 expression in ESL cells (Figure 1K). We then tested the differentiation potential of ESL cells. We showed that ESL cells could be induced to neuroectoderm cells expressing βIII-tubulin, a neuronal marker (Figure 1F) (Gaspard et al., 2009). We also tested whether ESL cells could differentiate into cell types indicative of the three germ layers. We generated differentiated embryoid bodies (Figure 1E) and obtained cardiac beating cells, and cells with expression of ACTA2 (mesoderm, Figure 1G), SOX1 (ectoderm, Figure 1I), and GATA4 (endoderm, Figure 1J). Similar differentiation potential was observed in vivo by transplanting ESL cells into mice to generate teratomas (Figures 1L–1N). Altogether the results validated our procedure for consistently generating ESL cell lines from GSCs and defined a baseline efficiency at which reprogramming occurred (~4 out of 100 wells; Table 1).

Exogenous OCT4 Promoted GSC Reprogramming by Upregulating CDH1

Although GSCs could reprogram to ESL cells consistently, the frequency was similarly low in our study as in studies by others (about 0.02% of cells plated). Interestingly, the presence of very high Oct4-GFP expression in a cluster of cells correlated with its ability to reprogram to ESL cells. Based on this observation, and the known role for OCT4 in pluripotency, we hypothesized that increasing OCT4 may increase the efficiency of GSC reprogramming. OCT4-inducible GSCs were established from doubly transgenic mice ("Dox-OCT4" and "Oct4-GFP") to study OCT4 function in GSC reprogramming. Dox-OCT4 transgenic mice expressed exogenous OCT4 in a doxycycline-dependent manner (Hochedlinger et al., 2005) (Figure 2A). In GSCs 1 μg/mL of doxycycline resulted in effective OCT4 overexpression (Figure 2B). Using our 48-well-plate reprogramming assay, we found a reproducible increase in the frequency of reprogramming when GSCs were cultured with doxycycline. This result suggested that OCT4 played a role in promoting GSC reprogramming (Figure 2C and Table 1).

The function of OCT4 in GSC reprogramming is still largely unknown. Interestingly, we noticed that ESL clusters appeared from within the middle of large clusters of GSCs (Figure 1C), indicating that the surrounding environment of cell-to-cell adhesion may influence reprogramming. It is known that CDH1 is required for the maintenance of cell-to-cell contacts in epithelial cells: anti-CDH1 antibodies can disrupt these contacts and induce a mesenchymal phenotype (Imhof et al., 1983). We found CDH1 increased after OCT4 induction (Figure 2D). In the presence of doxycycline, the highest levels of OCT4 were obtained from Dox-Oct4 homozygous mice, intermediate levels in Dox-Oct4 heterozygous mice, and low levels in wild-type mice. Accordingly, CDH1 protein increased as the amount of OCT4 increased, suggesting that *Cdh1* was a downstream gene of OCT4 and that OCT4's effect on reprogramming was mediated by CDH1. Indeed, OCT4 overexpression failed to induce GSC reprogramming when CDH1 was downregulated, indicating that the effect of OCT4 on reprogramming was dependent on CDH1 (Figure 2C and Table 1).

CDH1 is not only a surface marker on a subset of spermatogonia/SSCs but is also a typical marker of epithelial cells. We examined other epithelial markers including desmoplakin (*Dsp*) and crumbs family member 3 (*Crb3*) and found that they were also upregulated along with OCT4 (Figure 2E). Furthermore, cadherin 2 (*Cdh2*, also known as N-cadherin), a mesenchymal marker, was downregulated after OCT4 overexpression (Figure 2E). Increased epithelial and decreased mesenchymal markers indicated that GSCs may acquire properties of epithelial cells through MET during OCT4 induction. These results suggested that OCT4 promoted reprogramming in part by upregulating CDH1 and enabling GSCs to undergo MET.

MET Barrier Mediated by TGF-β Signaling Inhibits GSC Reprogramming

Recent studies have shown that conversion of fibroblasts into an intermediate epithelial cell is crucial during initiation of reprogramming (Li et al., 2010; Samavarchi-Tehrani et al., 2010). This phenotypic change occurs through induction of MET and is consistent with the fact that ESCs from the inner cell mass of the blastocyst are epithelial-like (Ocana and Nieto, 2010). It is known that SSC-containing populations of undifferentiated spermatogonia express both mesenchymal (THY1) and epithelial (CDH1) markers (Kubota et al., 2003; Tokuda et al., 2007). To gain better insight on the nature of GSCs, we quantitatively examined several mesenchymal/epithelial markers in direct comparison with ESCs. We found that mesenchymal markers including *Thy1* and *Cdh2* were expressed at higher levels in GSCs, while epithelial markers, including *Cdh1*, *Dsp*, *Pkp1*, and *Crb3*, were expressed at lower levels in GSCs (Figures 3A and 3C). These results were consistent with recently published RNA-seq data (Liu et al., 2016) and suggested that GSCs favor the mesenchymal state over the epithelial state.

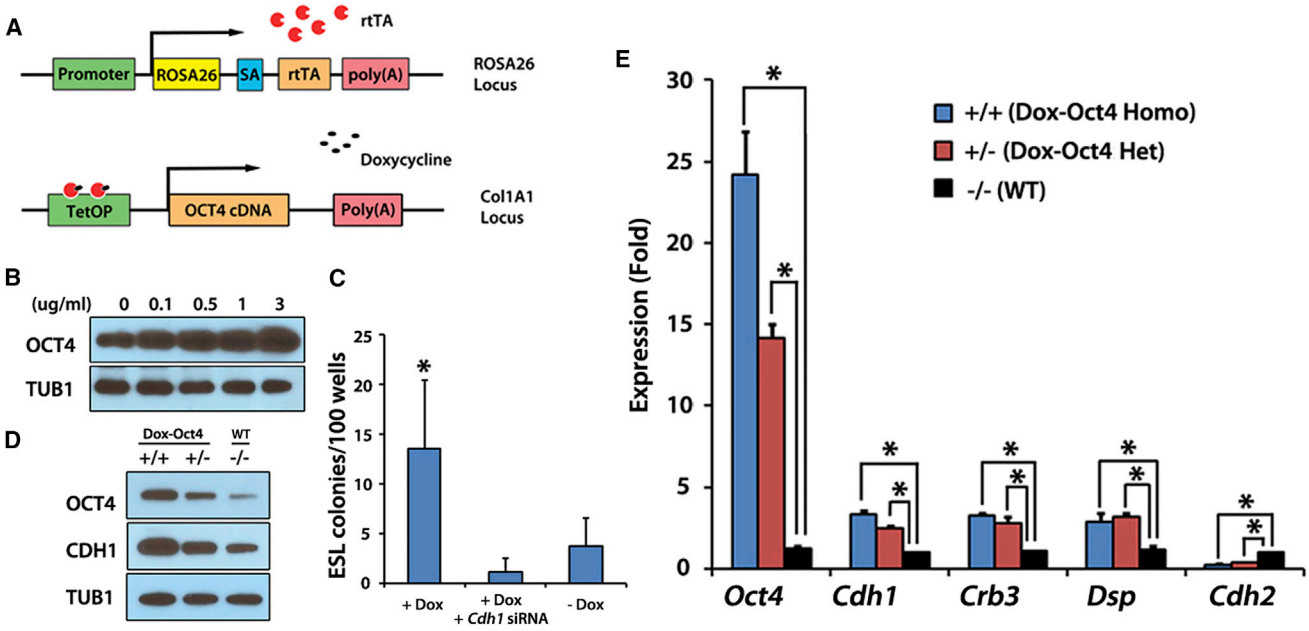

Figure 2. Doxycycline-Dependent OCT4 Overexpression Promotes GSC Reprogramming

(A) Schematic representation of Dox-Oct4 transgenic mice. The rtTA gene was targeted into the ROSA26 locus under control of the ROSA promoter. A cassette containing the *Oct4* cDNA under the control of the doxycycline-responsive promoter was inserted downstream of the collagen locus. SA, splice acceptor; TetOP, tetracycline/doxycycline-responsive operator. Black arrows indicate transcriptional start sites.

(B) OCT4 (top) and TUB1 (bottom) immunoblotting of GSC lysates from Dox-Oct4 homozygous mice treated with different concentrations of doxycycline.

(C) GSC reprogramming efficiency in RP medium after 1 μg/mL doxycycline treatment (n = 96 wells total from six experiments) compared with doxycycline and *Cdh1* siRNA co-treatment group (n = 96 wells total from four experiments) and untreated control group (n = 96 wells total from five experiments). *p < 0.01, significance between doxycycline-only group and each of the other two groups. The values in the histogram are presented as the means ± SD.

(D) OCT4 (top), CDH1 (middle), and TUB1 (bottom) immunoblotting of cells lysates from homozygotes (+/+), heterozygotes (+/−), and wild-type (−/−) GSCs after 72 hr of doxycycline treatment (1 μg/mL).

(E) qRT-PCR analysis of mesenchymal or epithelial marker expression as indicated. RNA was isolated from Dox-Oct4 homozygotes (+/+), Dox-Oct4 heterozygotes (+/−), and wild-type (−/−) GSCs after 1 μg/mL of doxycycline treatment (72 hr). The values in the histogram are presented as the means ± SD. Mean and SD for three biological replicates from three independent experiments are shown. *p < 0.01.

Transforming growth factor β (TGF-β) signaling plays a major role in influencing MET (Akhurst and Hata, 2012). TGF-β induces EMT through SMAD-mediated and SMAD-independent signaling. In SMAD-mediated signaling TGF-β signals through a tetrameric complex of receptors to activate SMAD2 and SMAD3 and turns on expression of EMT-related factors. Consistent with our observations showing that GSCs exhibit an EMT-favored (mesenchymal) state, we found evidence for relatively higher TGF-β signaling in GSCs than in ESCs. Specifically, *Tgfbr1* and phosphorylated SMAD3 were much higher in GSCs than ESCs (Figures 3B and 3C). Also, *Smad7*, a negative regulator of TGF-β signaling, was lower in GSCs than in ESCs (Figure 3B). These results showed that TGF-β signaling, which plays a negative role in MET, was activated in GSCs. We analyzed factors known to induce EMT, such as *Zeb1*, *Zeb2*, *Twist1*, *Twist2*, *Snai1*, and *Slug*, and found that they were also more highly expressed in GSCs compared with ESCs (Figure 3B). Altogether, a high expression of negative regulators of MET established a MET barrier for GSCs.

We hypothesized that breaking the MET barrier may help to increase the efficiency of GSC reprogramming. To test this prediction we used the TGFBR1 inhibitors, RepSox and SB431542, to repress TGF-β signaling. Treatment of GSCs for 3 days led to decreased phosphorylated SMAD3 (Figure 3C) and increased *Smad7* (Figure 3D), confirming the effectiveness of each inhibitor treatment (Figure 3C). Also, repressors of MET, *Zeb1* and *Snai1*, were decreased by RepSox treatment while factors associated with MET, SOX2 and CDH1, were upregulated (Figures 3C and 3D) (Li et al., 2010). In addition, OCT4 and NANOG were increased by 3 days of RepSox treatment (Figure 3C). Importantly, when RepSox treatment was added to

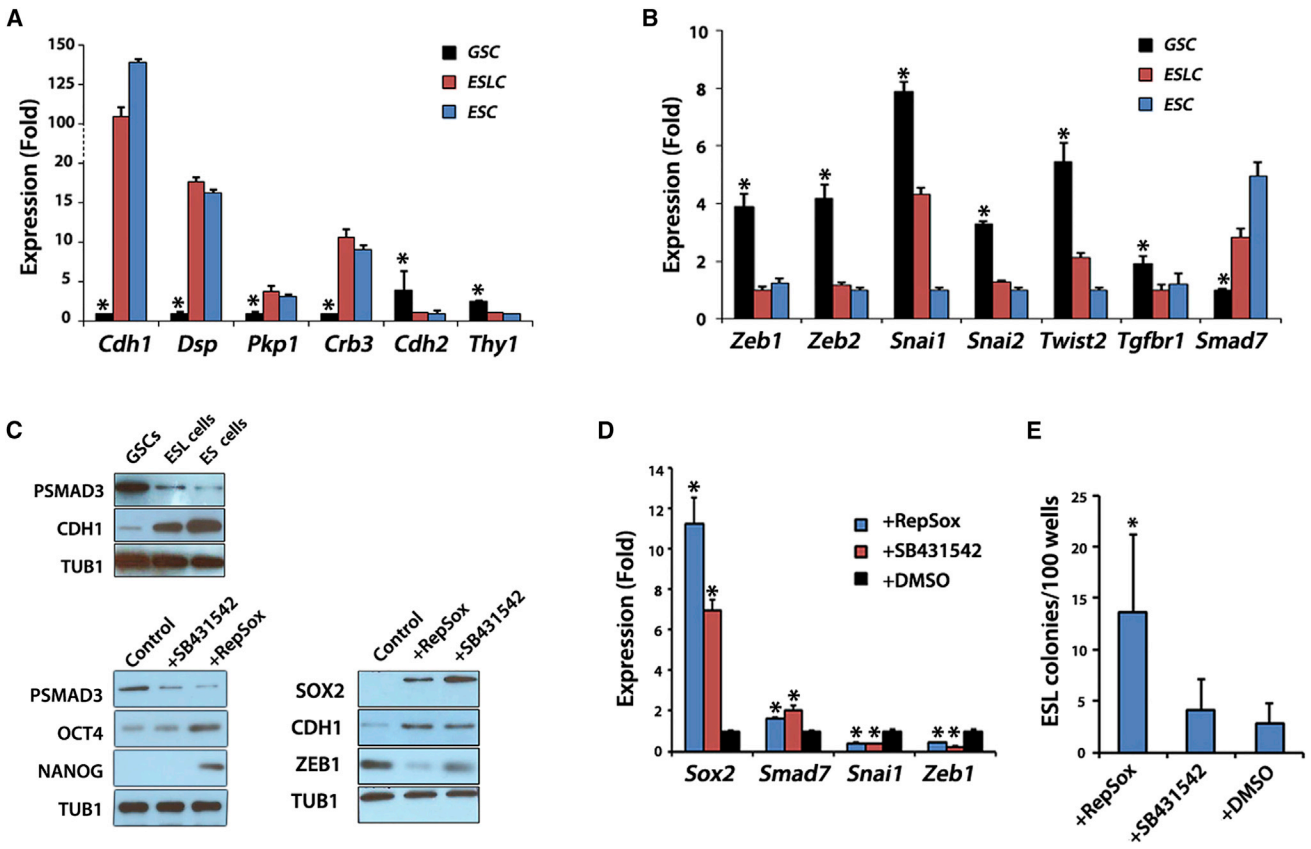

Figure 3. Effect of TGF-β Signaling-Mediated Modulation of MET on GSCs Reprogramming

(A and B) qRT-PCR analysis of mesenchymal/epithelial markers (A) and MET regulators (B) as indicated. RNAs were from Oct4-GFP GSCs, ESL cells, and ES-D3 cells. *$p < 0.01$.

(C) Top: phospho-SMAD3, CDH1, and TUB1 immunoblotting of cells lysates from GSCs, ESL cells, and ES-D3 cells. Bottom: phospho-SMAD3, OCT4, NANOG, SOX2, CDH1, ZEB1, and TUB1 immunoblotting of cell lysates from GSCs treated with 25 μM RepSox, 25 μM SB431542, or DMSO (Control).

(D) qRT-PCR analysis of mesenchymal/epithelial-related genes in RNAs of GSCs after 72 hr of treatment with 25 μM RepSox and 25 μM SB431542. DMSO was used as control. *$p < 0.01$.

(E) GSC reprogramming efficiency in RP medium after TGF-β signaling inhibitor (n = 144 wells from seven experiments for RepSox, n = 84 wells from four experiments for SB431542) compared with DMSO control (n = 144 wells from six experiments). *$p < 0.01$.

In (A), (B), (D), and (E), the values in the histograms are presented as the means ± SD. Mean and SD for three biological replicates from three independent experiments are shown.

reprogramming medium, we saw a marked increase in reprogramming efficiency (Figure 3E and Table 1). However, SB431542 failed to promote GSC reprogramming for reasons that are unclear. One possibility is that both RepSox and SB431542 upregulated CDH1 and increased CDH1$^+$ cells after 3 days; however, SB431542-treated cells failed to maintain elevated CDH1 after 2 weeks of treatment (Figure S2). In addition, unlike with RepSox, cells treated with SB431542 did not have upregulated OCT4 or NANOG or substantially downregulated ZEB1 (Figure 3C). ESL cells generated with RepSox treatment were confirmed to have pluripotent properties based on their ability to form teratomas (Figure S3). These results support the idea of a MET barrier that prevents GSCs from acquiring pluripotency, and that repressing TGF-β signaling could boost MET and promote GSC reprogramming.

ZEB1 but Not ZEB2 Is a MET Regulator in GSC Reprogramming

The process of MET represents a reversion of EMT; therefore, one might predict that downregulation of EMT-inducing transcription factors, such as ZEB1, ZEB2, and TWIST2, would promote GSC reprogramming by promoting MET. We tested this idea by knocking down *Zeb1*, *Zeb2*, and *Twist2* using small interfering RNA (siRNA) transfection. *Zeb1*, *Zeb2*, and *Twist2* mRNA

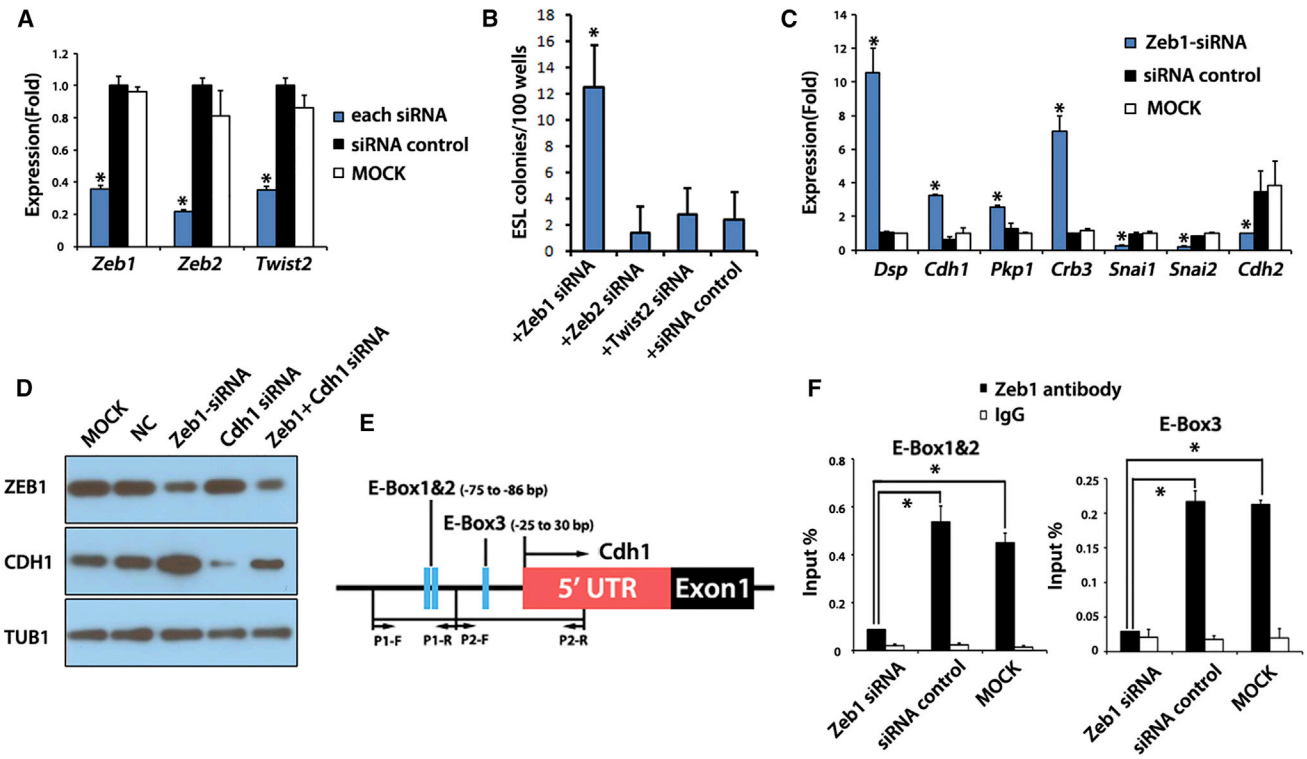

Figure 4. ZEB1 Represses MET through Binding to the *Cdh1* Promoter in GSCs

(A) qRT-PCR analysis of RNAs from GSCs treated with *Zeb1*, *Zeb2*, and *Twist2* siRNA for 72 hr. *Zeb1*, *Zeb2*, and *Twist2* genes were detected. *$p < 0.01$, significant difference between siRNA and each control separately.

(B) GSC reprogramming efficiency in RP medium after *Zeb1* siRNA (n = 192 total wells from nine experiments), *Zeb2* siRNA (n = 84 total wells from five experiments), and *Twist2* siRNA (n = 84 total wells from five experiments) treatment. Scrambled non-targeting siRNA was used as a control (n = 168 total wells from nine experiments). *$p < 0.01$.

(C) The expression of MET-related genes after *Zeb1* siRNA treatment. qRT-PCR analysis of mesenchymal/epithelial-related genes in GSCs treated with *Zeb1* siRNA. siRNA consisting of a scrambled sequence was used as negative control (NC). GSCs without siRNA transfection were used as control (MOCK). *$p < 0.01$, significant difference between siRNA and each control separately.

(D) ZEB1 (top), CDH1 (middle), and TUB1 (bottom) immunoblotting of GSC lysates treated with different siRNA combinations. siRNA consisting of a scrambled sequence was used as negative control (NC).

(E) The locations of E boxes and primers in CDH1 gene promoter (small arrows). Black arrow indicates the transcriptional start site.

(F) qPCR analysis of DNAs from GSCs after chromatin immunoprecipitation (ChIP) by using ZEB1 antibody. ChIP was performed using GSCs treated with *Zeb1* siRNA, control siRNA (NC), or no siRNA (MOCK) and qPCR was used to analyze the E-box 1/2 and E-box 3 in the promoter of CDH1. Enrichment is presented as (ChIP/input) × 100.

In (A), (B), (C), and (F), the values in the histograms are presented as the means ± SD. Means and SD for three biological replicates from three independent experiments are shown. *$p < 0.01$.

levels in GSCs were significantly reduced after each siRNA treatment (Figure 4A). To test whether ZEB1 influenced MET in GSCs, we determined expression of MET genes in GSCs after siRNA treatment (Figure 4C). *Zeb1* knockdown led to a significant increase in *Cdh1*, *Dsp*, *Pkp1*, and *Crb3* and a decrease in *Snai1*, *Snai2*, and *Cdh2*. Interestingly, *Zeb1* knockdown, but not *Zeb2* or *Twist2* knockdown, promoted GSC reprogramming (Figure 4B and Table 1), suggesting that not all EMT-inducing factors functioned as barriers for GSC reprogramming.

CDH1 is one of the defining features of the epithelial state (Zeisberg and Neilson, 2009). As described above, our results showed that CDH1 was necessary in GSC reprogramming regulated by OCT4. To test whether CDH1 was also involved in ZEB1-regulated GSC reprogramming, we co-transfected *Zeb1* and *Cdh1* siRNA during reprogramming. Without CDH1 reprogramming was virtually undetectable in our assay (Table 1), suggesting that CDH1 was a crucial factor in GSC reprogramming and that CDH1 may be downstream of ZEB1 regulation. Consistent with this idea, western blotting showed that *Zeb1* knockdown

increased CDH1 but not the opposite (Figure 4D). These results suggested *Zeb1* knockdown promoted GSC reprogramming via CDH1.

The 5′ proximal promoter region of *Cdh1* contains E boxes, sites for direct binding of specific transcription regulators. E boxes in the mouse *Cdh1* promoter were shown to play a crucial role in the epithelial-specific expression of *Cdh1* (Behrens et al., 1991; Giroldi et al., 1997). To test whether ZEB1 directly regulated CDH1 expression, we analyzed three E-box elements in the promoter of CDH1 by chromatin immunoprecipitation (ChIP) using a ZEB1 antibody (Figure 4E). qPCR analysis of the immunoprecipitated DNA showed that ZEB1 could bind to all three E boxes (Figure 4F). The binding was reduced when ZEB1 was knocked down. These results showed that ZEB1 directly regulated *Cdh1* expression and suggested that ZEB1 inhibits MET in GSCs by directly repressing CDH1 transcription.

A Rare Population of Epithelial-like GSCs Exhibits Enhanced Reprogramming Ability

Undifferentiated spermatogonia, and likewise GSC populations, are known to be heterogeneous, with different subpopulations expressing different combinations of proteins (Dann et al., 2008; Hermann et al., 2015; Niedenberger et al., 2015). As shown by immunoblotting (Figure 3C), CDH1 is detected weakly in the GSC population. We hypothesized that a subset of GSCs with elevated CDH1 may exhibit enhanced reprogramming ability. When using collagenase type II to dissociate cells prior to immunostaining and flow cytometry, CDH1 expression was detected in ~60% of GSCs and with a range of expression levels. In contrast, consistent with the known sensitivity of CDH1 epitopes to trypsin, trypsin-digested GSCs exhibited a much lower percentage of $CDH1^+$ cells (~3%) (Figure S4). Interestingly, the rare $CDH1^+$ cells detected after trypsin digestion showed significantly higher reprogramming efficiency than $CDH1^-$ cells (Table 1 and Figure 5E), suggesting that this $CDH1^+$ cell population has unique properties. Therefore, we focused on the properties of these rare $CDH1^+$ cells that remained after trypsin digestion (hereafter, $CDH1^+$).

To further understand the properties of $CDH1^+$ GSCs and $CDH1^-$ GSCs, we used flow cytometry to sort the two populations after trypsin digestion and compared them by total RNA-seq. A total of 23,803 transcripts were detected, of which 3,125 were upregulated (red in Figure 5A) and 2,134 were downregulated (green in Figure 5A) in $CDH1^+$ GSCs compared with $CDH1^-$ GSCs (fold change>2). The differentially transcribed genes (fold change>2) were classified into 28 gene ontology terms, including 13 biological processes, seven cellular components, and eight molecular functions (Figure S5). The data clearly showed $CDH1^+$ and $CDH1^-$ cells as having highly distinct profiles (Figure 5B). In particular, numerous epithelial genes (e.g., *Dsp*, *Pkp2*, and *Krt19*) and pluripotency factors (*Nanog* and *Sox2*) were highly expressed in the $CDH1^+$ population. In contrast, most genes known to be general markers of SSCs/undifferentiated spermatogonia were downregulated (e.g., *GFRA1* and *ID4*) or unchanged (e.g., *ZBTB16 and SALL4*) in $CDH1^+$ GSCs (Figures 5A and 5C). KEGG pathway analysis revealed that the populations exhibited distinct activity in signaling pathways including WNT and TGF-β signaling (Figure S5). Notably, *Tgfbr1*, *Smad2*, and *Smad3* tended to be lower in $CDH1^+$ GSCs while *Smad7*, an inhibitor of TGF-β signaling, was higher. qRT-PCR analysis confirmed that these trends were statistically significant and showed that epithelial markers *Cdh1*, *Dsp*, and *Crb3* were highly expressed whereas mesenchymal markers *Thy1*, *Cdh2*, *Zeb1*, and *Zeb2* were lowly expressed in $CDH1^+$ GSCs (Figure 5D). The results showed that $CDH1^+$ GSCs were more epithelial in nature compared with $CDH1^-$ GSCs and supported the notion that $CDH1^+$ GSCs are able to partly overcome the MET barrier because they may be in an advanced stage of MET.

$CDH1^+$ GSCs were quantified at different time points during GSC reprogramming. We found that $CDH1^+$ GSCs increased over the weeks of reprogramming (Figure 5G), supporting the idea that upregulation of CDH1 through MET occurs during GSC reprogramming. Interestingly, *Zeb1* siRNA and RepSox, treatments that both enhanced reprogramming efficiency, also resulted in increased $CDH1^+$ GSCs 2 weeks into reprogramming (Figures S2, S4, and S6), indicating that ZEB1 and TGF-β signaling inhibited the upregulation of CDH1. In summary, these results showed that MET was a crucial step in GSC reprogramming and by initiating reprogramming with rare trypsin-resistant $CDH1^+$ GSCs the barrier to reprogramming was reduced, because $CDH1^+$ GSCs were poised in a later stage of MET.

For obtaining autologous testes-derived pluripotent cells from patients, it is likely that direct reprogramming from primary testicular cells would be required instead of establishing GSC lines. To study whether MET also plays a role in reprogramming of SSCs obtained directly from the testes, we sorted $THY1^+$ cells (enriched in SSCs) from Oct4-GFP mice testes and quantified their reprogramming ability. $THY1^+$ cells were directly sorted into wells in 48-well plates and treated with RepSox and *Zeb1* siRNA for 6 weeks. Similar to results obtained with GSCs, testicular SSCs treated with RepSox or *Zeb1* siRNA showed increased SSC reprogramming efficiency (Table 1). Using sorted $CDH1^+$/$THY1^+$ SSCs also promoted cell reprogramming efficiency (Table 1). These results suggested that methods based on overcoming a MET barrier were not only relevant to

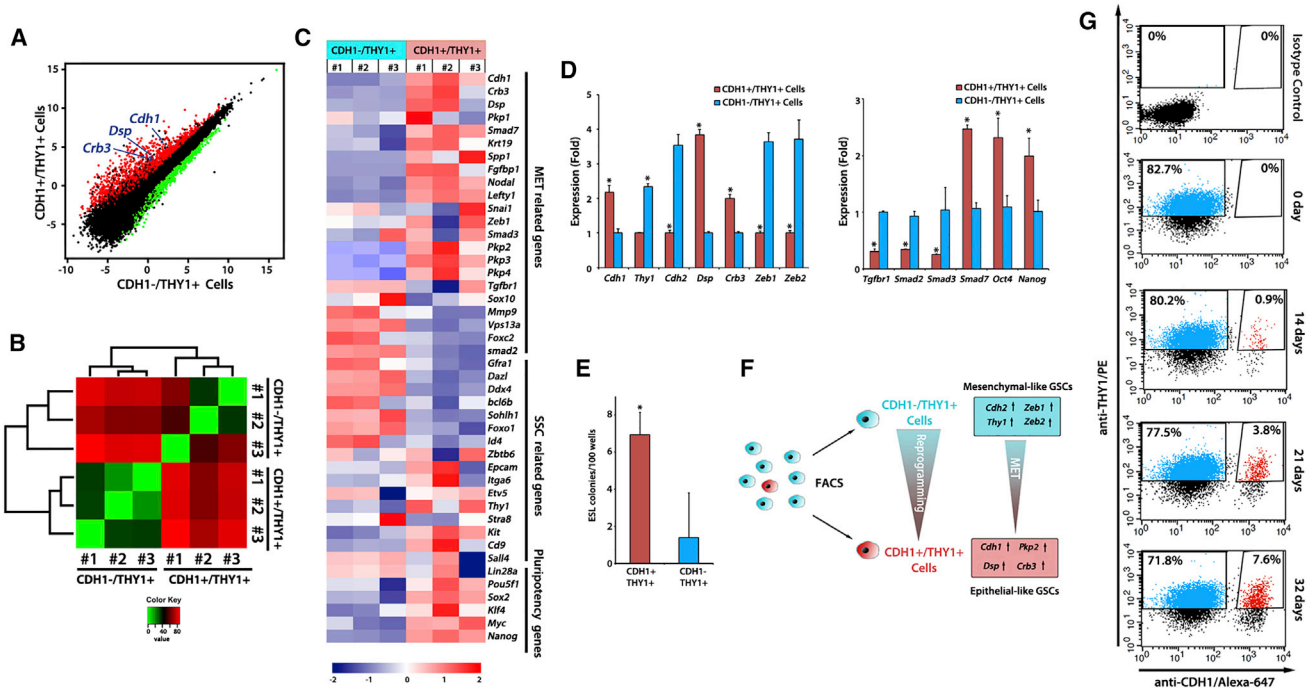

Figure 5. CDH1 Defines an Epithelial-like GSC Subpopulation with Enhanced Reprogramming Efficiency

(A) Pairwise comparison of expression profiles for CDH1$^-$/THY1$^+$ and CDH1$^+$/THY1$^+$ cells. The scatterplot represents normalized expression values (average fragments per kilobase of transcript per million mapped reads) of individual genes, with the genes increased or decreased >2-fold in CDH1$^-$/THY1$^+$ and CDH1$^+$/THY1$^+$ cells indicated in red and green, respectively. *Crb3*, *Dsp*, and *Cdh1* are marked in blue.

(B) Heatmap showing the hierarchically clustered correlation matrix resulting from comparing the transcript expression values for each pair of samples.

(C) Heatmap showing the relative expression levels of each sample.

(D) qRT-PCR analysis of MET-related gene expression in CDH1$^+$/THY1$^+$ and CDH1$^-$/THY1$^+$ cells. The values in the histogram are presented as the means ± SD. Means and SD for three biological replicates from three independent experiments are shown. *$p < 0.01$.

(E) Reprogramming efficiency in RP medium by using CDH1$^-$/THY1$^+$ cells (n = 96 wells from three experiments) and CDH1$^+$/THY1$^+$ cells (n = 88 wells from three experiments). The values in the histogram are presented as the means ± SD. *$p < 0.01$.

(F) Schematic representation summarizing sorting experiment and results.

(G) Flow cytometry analysis of CDH1 and THY1 expression in GSC (wild-type) reprogramming at indicated time points. Forward and side scatterplots were used to define viable GSCs (not shown) and isotype controls were used to define positive immunostaining. Percentage of parent gates are indicated with CDH1$^+$/THY1$^+$ cells marked in red.

GSC reprogramming but also promoted testicular SSC reprogramming.

DISCUSSION

SSCs are unique among adult cell types in that they share expression of many mRNAs in common with ESCs, including all four Yamanaka factors. Although levels are lower compared with ESCs, *Oct4*, *Klf4*, and *Myc* mRNA and protein, and *Sox2* mRNA are all expressed in SSCs, implying that SSCs may contain special protective mechanisms to prevent acquisition of pluripotency in the germline and that additional factors may be required for the initiation of SSC reprogramming (Kanatsu-Shinohara et al., 2008). Our results show that relatively high expression of ZEB1, along with relatively high TGF-β signaling in GSCs compared with ESCs, play a pivotal role in preventing MET in GSCs, thereby inhibiting their reprogramming to pluripotency (Figure 6). We show that enhanced reprogramming can be achieved with three general approaches and that each approach is correlated with an increase in the CDH1$^+$ cell population. First, knockdown of *Zeb1*, but not *Zeb2* or *Twist2*, enhances reprogramming through its effect on CDH1. Second, RepSox treatment, but not SB431542 treatment, results in a greater CDH1$^+$ cell population while increasing reprogramming efficiency. Finally, using isolated CDH1$^+$ cells directly for reprogramming enhances the generation of ESL cells while CDH1$^-$ cells exhibit reprogramming efficiency lower than

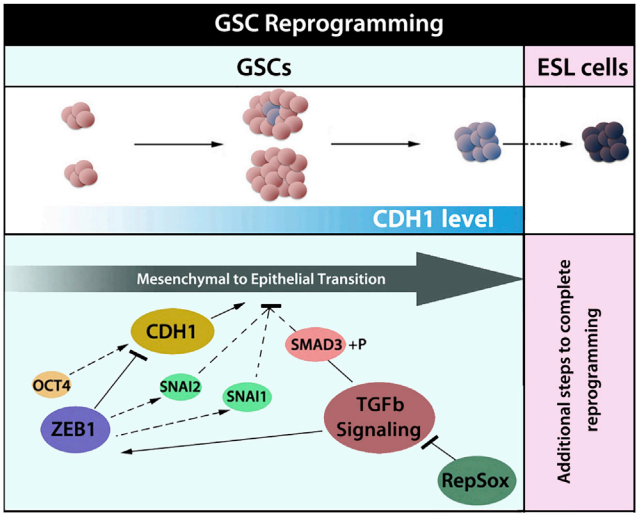

Figure 6. Model of Mechanistic Regulation of Mesenchymal to Epithelial Transition in Reprogramming

Initially, GSCs have moderate to no detectable CDH1 expression. During prolonged culturing rare, transitional GSCs emerge with higher CDH1, reflecting an initiation of MET. Additional known and unknown factors (pink box) further drive reprogramming of MET transitional colonies to a fully epigenetically reprogrammed state of pluripotency. OCT4 and ZEB1 and TGF-β signaling regulate MET during SSC reprogramming. ZEB1 regulates Snai1/2 and directly represses CDH1 expression, thereby preventing MET.

the basal level of spontaneous reprogramming observed in controls.

MET is an important step in reprogramming fibroblasts to iPSCs (Li et al., 2010; Samavarchi-Tehrani et al., 2010), and the acquisition of epithelial features and loss of mesenchymal features are known to occur soon after transfection with Yamanaka factors (David and Polo, 2014; Polo et al., 2012). Traditionally, SSCs have been considered neither mesenchymal nor epithelial. Extensive genomic profiling of neonatal mouse spermatogonia recently suggested that both epithelial-like and mesenchymal-like subpopulations of spermatogonia were present (Hammoud et al., 2015). Similarly, we found that GSCs in vitro comprise both epithelial-like ($CDH1^+$) and mesenchymal-like ($CDH1^-$) cells. However, side-by-side comparisons with ESCs show that the GSC population appears to be dominated by a mesenchymal phenotype because expression of epithelial markers, such as *Cdh1*, *Crb3*, and *Dsp*, are much lower in GSCs than ESCs. In addition, GSCs exhibit high expression of MET repressors such as ZEB1, ZEB2, and TWIST2, factors that one would expect to further reinforce the mesenchymal phenotype and prevent acquisition of pluripotency by GSCs. We demonstrate that ZEB1, although not ZEB2 or TWIST2, is a key contributor to the MET barrier that prevents GSC conversion to pluripotency (Figure 6). ZEB1 is well known as an inducer of EMT, the opposite process of MET (Li et al., 2014; Shu and Pei, 2014). ZEB1 has been shown to act as a direct transcriptional repressor of CDH1 in a variety of cell types, but to our knowledge a role for ZEB1 in SSCs has not been described (Eger et al., 2005; Grooteclaes and Frisch, 2000). We provide evidence here that in GSCs ZEB1 directly binds the *Cdh1* promoter at both the E-box 1/2 and E-box 3 regions, and that loss of ZEB1 results in increased CDH1 expression and a reduction in the barrier to SSC and GSC reprogramming to pluripotency.

CDH1 is one of the defining marks of the epithelial state. Ironically, CDH1 and THY1 have both been commonly used as spermatogonial markers. We noticed that although THY1 expression is abundant, GSCs have overall much lower expression of CDH1 than ESCs. Only about 3% of GSCs were $CDH1^+$ after trypsin digestion (Figure S4), but after collagenase type II digestion a much higher fraction of GSCs (~60%) were $CDH1^+$. In contrast, ESCs were over 80% $CDH1^+$, even after trypsin digestion (J.A., unpublished data). Others have used collagenase type II instead of trypsin for testis digestion before CDH1 cell sorting, presumably to protect CDH1 epitopes. Altogether, the results suggested that by using trypsin the sensitivity of our flow cytometry assay was reduced such that only those GSCs with highest CDH1 expression could be detected. In support of this idea, following collagenase type II digestion gene expression analysis of the 3% highest expressing CDH1 cells exhibited relatively high *Crb3*, *Dsp*, and *Nanog* and low *Cdh2* and *Zeb1*, patterns comparable with the $CDH1^+$ trypsin-digested cells (Figure S7). Also, after RepSox or *Zeb1* siRNA treatment, comparable effects were observed regardless of the enzyme used for cell dissociation (Figure S4). Hence, despite differences in the absolute number of $CDH1^+$ cells observed with different methods of cell preparation, the GSC subpopulation with the highest CDH1 expression appears to correspond to cells with epithelial properties that are poised in a later stage of MET and with greatest potential for reprogramming.

Transcriptome-wide analysis of the rare $CDH1^+$ trypsin-digested GSC population revealed that they have an epithelial gene expression profile, suggesting that GSC-derived ESL cells may originate from these epithelial-like cells. By using the trypsin-digested $CDH1^+$ and $CDH1^-$ cells to initiate a reprogramming experiment it was apparent that the $CDH1^+$ population had a higher reprogramming efficiency than $CDH1^-$ cells. The results further support a model wherein MET presents a barrier to GSC reprogramming that can be overcome by selecting cells that have already acquired epithelial characteristics, possibly because they are already undergoing MET, to initiate reprogramming. Still, lineage tracing would be required to prove that cells that upregulate CDH1 are the origin of ESL cells.

Interestingly, not only do the CDH1$^+$ GSCs exhibit gene expression consistent with MET, they also are highly enriched in multiple pluripotency factors, including *Nanog*, an important pluripotency factor not previously detected in SSCs or GSCs. In the context of the normal GSC reprogramming procedure, it is likely that the prolonged culturing of clusters leads to a microniche as proposed by Ko et al. (2010) that is defined by acquisition of epithelial features conducive to the conversion to pluripotency.

Previous studies of GSC reprogramming commonly utilized genetically modified mice. For instance, Oct4-GFP mice have been used because they provide a convenient way to monitor the process of reprogramming (Ko et al., 2010; Youn et al., 2013). Using transgenic mice may be precluded in certain research contexts and is not applicable to clinical settings. We show that the use of *Zeb1* knockdown and RepSox are effective for increasing reprogramming efficiency. Both approaches are effective in mice with other genetic backgrounds including C57BL6 wild-type mice, and the experimental approach does not depend on visualization of an Oct4-GFP reporter. ESL cells generated in our study, including from four conditions (RP medium control, RP medium with Dox, RP medium with RepSox, and RP medium with *Zeb1* siRNA) exhibit many characteristics of pluripotent cells, including the ability to differentiate to mesoderm, ectoderm, and endoderm both in vitro and in a teratoma assay (Figures 1 and S3). It should be noted, however, that the ESL lines generated in our study were not tested for ability to contribute to a chimera following injection into blastocysts, so conclusions about the extent of pluripotency are tentative. Still, the baseline reprogramming culture conditions and techniques used here (i.e., RP medium control) were proved to generate bona fide pluripotent ESL cells with chimera-forming ability by others (Ko et al., 2009).

In recent years a variety of technologies have emerged for the generation of pluripotent cells, each of which may have its own benefits. Pluripotent cell lines generated by each method may be particularly suitable for certain downstream applications, and it is known that even individual cell lines generated from the same method may exhibit variable propensity for subsequent differentiation. In some cases, using germ cell-derived pluripotent cells may be advantageous over somatic cell-derived pluripotent cells. ESL cells are more equivalent to ESCs than iPSCs of somatic origin in terms of gene expression profiles, indicating that ESL cells might be better than iPSCs for therapeutic purposes (Ko et al., 2009). Also, the presence of telomerase activity in SSCs may lend itself to the production of superior cells for transplantation-based therapies (Ozturk, 2015; Pech et al., 2015). Finally, the ability to obtain pluripotent cells spontaneously, without introducing transgenes, provides advantages. Ultimately, further research will be needed to determine the ideal source of pluripotent cells for any given application.

Some reports have claimed that human SSCs may also become spontaneously reprogrammed to pluripotency; however, more recent data suggest that the cell lines that were generated are fibroblast-like in nature and may be related to multipotent mesenchymal-like stem cells, not ESL cells (Chikhovskaya et al., 2014; Ko et al., 2011; Kossack et al., 2009; Zheng et al., 2014). Based on our observations here with mouse SSCs, it may be possible to obtain bona fide germ cell-derived ESL cells from human testes by enriching for epithelial-like spermatogonia and/or promoting MET through manipulation of TGF-β signaling.

EXPERIMENTAL PROCEDURES

Mice

Transgenic mice were from The Jackson Laboratory. "Dox-Oct4" mice are B6;129-Gt(ROSA)26Sortm1(rtTA*M2)Jae Col1a1tm2 (tetO-Pou5f1)Jae/J (Stock No. 006911). "Oct4-GFP" mice are B6;CBA-Tg(Pou5f1-EGFP)2Mnn/J (Stock No. 04654) and are also known as OG2. Dox-Oct4 homozygous and Oct4-GFP mice were intercrossed to generate doubly transgenic mice. Wild-type mice were C57BL6 background. All procedures involving mice were approved by the Bloomington Institutional Animal Care and Use Committee.

Reprogramming Assay

In initial experiments we determined that plating 200–400 cells per well of a 48-well plate, with minimally 12 replicates, produced an ideal density and quantity of cells to reliably observe reprogramming in at least one well. For the experiments in this study, established GSCs (around passage 6) were seeded on DR4 MEFs at a low density of 250 cells (or 500 cells for primary testis SSCs) per one well of a 48-well plate (Falcon). Cells were fed with RP medium (Table S4) at least two times per week and maintained without passaging until ESL cell colonies appeared, generally 5–7 weeks after seeding. Using this procedure only a single ESL colony could be discerned in any given well. For quantification of wells with ESL cells, all wells of cells were dissociated with 0.05% trypsin and replated (one to one) into new wells with ES medium (Table S4). Wells were scored based on whether the trypsinized cells could proliferate rapidly following trypsinization and transfer to ES medium. Since GSCs require GDNF for proliferation, and ES medium lacks GDNF, remaining germ cells that did not undergo reprogramming died following transfer to the new well. Hence, each well was scored as either positive (ESL cells grew) or negative (cells died). Data from reprogramming assays are summarized in Table 1.

Statistical Analysis

Experiments including qRT-PCR, western blot, and ChIP assay were repeated at least three times ($n > 3$) with different individual samples (biological replicates). More than 12 wells ($n > 12$) per treatment group were set up for a single GSC reprogramming experiment and each experiment was reproduced at least three

times. Total number of wells and experimental replicates for reprogramming are summarized in Table 1 and provided individually in the figure legends. The values in each histogram (qRT-PCR, ChIP-PCR, and reprogramming) are presented as the means ± SD. Significant differences between means of biological replicates were compared pairwise using Student's t test.

ACCESSION NUMBERS

The accession number for the RNA sequencing data reported in this paper is GEO: GSE90712.

SUPPLEMENTAL INFORMATION

Supplemental Information includes Supplemental Experimental Procedures, seven figures, and four tables and can be found with this article online at http://dx.doi.org/10.1016/j.stemcr.2016.12.006.

AUTHOR CONTRIBUTIONS

J.A. designed and performed experiments, analyzed data, and wrote the manuscript; Y.Z. performed experiments and analyzed data; C.T.D. conceived and supervised the study, analyzed data, and wrote the manuscript.

ACKNOWLEDGMENTS

Thank you to Aaron Michael Buechlein, Christiane Hassel, and Sue Childress for technical assistance. Indiana University Bloomington Center for Genomics and Bioinformatics and Flow Cytometry Core Facilities were used for certain experiments. Research was supported by funding from the Eunice Kennedy Shriver National Institute of Child Health and Human Development of the NIH under award number 4R01HD071081.

Received: September 11, 2016
Revised: December 5, 2016
Accepted: December 6, 2016
Published: January 5, 2017

REFERENCES

Akhurst, R.J., and Hata, A. (2012). Targeting the TGF beta signalling pathway in disease. Nat Rev. Drug Discov. *11*, 790.

Behrens, J., Lowrick, O., Klein-Hitpass, L., and Birchmeier, W. (1991). The E-cadherin promoter: functional analysis of a G.C-rich region and an epithelial cell-specific palindromic regulatory element. Proc. Natl. Acad. Sci. USA *88*, 11495–11499.

Chikhovskaya, J.V., van Daalen, S.K.M., Korver, C.M., Repping, S., and van Pelt, A.M.M. (2014). Mesenchymal origin of multipotent human testis-derived stem cells in human testicular cell cultures. Mol. Hum. Reprod. *20*, 155–167.

Dann, C.T., Alvarado, A.L., Molyneux, L.A., Denard, B.S., Garbers, D.L., and Porteus, M.H. (2008). Spermatogonial stem cell self-renewal requires OCT4, a factor downregulated during retinoic acid-induced differentiation. Stem Cells *26*, 2928–2937.

David, L., and Polo, J.M. (2014). Phases of reprogramming. Stem Cell Res. *12*, 754–761.

Eger, A., Aigner, K., Sonderegger, S., Dampier, B., Oehler, S., Schreiber, M., Berx, G., Cano, A., Beug, H., and Foisner, R. (2005). DeltaEF1 is a transcriptional repressor of E-cadherin and regulates epithelial plasticity in breast cancer cells. Oncogene *24*, 2375–2385.

Fanslow, D.A., Wirt, S.E., Barker, J.C., Connelly, J.P., Porteus, M.H., and Dann, C.T. (2014). Genome editing in mouse spermatogonial stem/progenitor cells using engineered nucleases. PLoS One *9*, e112652.

Gaspard, N., Bouschet, T., Herpoel, A., Naeije, G., van den Ameele, J., and Vanderhaeghen, P. (2009). Generation of cortical neurons from mouse embryonic stem cells. Nat. Protoc. *4*, 1454–1463.

Ginsburg, M., Snow, M.H., and McLaren, A. (1990). Primordial germ cells in the mouse embryo during gastrulation. Development *110*, 521–528.

Giroldi, L.A., Bringuier, P.P., de Weijert, M., Jansen, C., van Bokhoven, A., and Schalken, J.A. (1997). Role of E boxes in the repression of E-cadherin expression. Biochem. Biophys. Res. Commun. *241*, 453–458.

Grooteclaes, M.L., and Frisch, S.M. (2000). Evidence for a function of CtBP in epithelial gene regulation and anoikis. Oncogene *19*, 3823–3828.

Guan, K., Nayernia, K., Maier, L.S., Wagner, S., Dressel, R., Lee, J.H., Nolte, J., Wolf, F., Li, M.Y., Engel, W., et al. (2006). Pluripotency of spermatogonial stem cells from adult mouse testis. Nature *440*, 1199–1203.

Hammoud, S.S., Low, D.H., Yi, C., Lee, C.L., Oatley, J.M., Payne, C.J., Carrell, D.T., Guccione, E., and Cairns, B.R. (2015). Transcription and imprinting dynamics in developing postnatal male germline stem cells. Genes Dev. *29*, 2312–2324.

Heim, C.N., Fanslow, D.A., and Dann, C.T. (2012). Development of quantitative microscopy-based assays for evaluating dynamics of living cultures of mouse spermatogonial stem/progenitor cells. Biol. Reprod. *87*, 90.

Hermann, B.P., Mutoji, K.N., Velte, E.K., Ko, D.J., Oatley, J.M., Geyer, C.B., and McCarrey, J.R. (2015). Transcriptional and translational heterogeneity among neonatal mouse spermatogonia. Biol. Reprod. *92*, 54.

Hochedlinger, K., Yamada, Y., Beard, C., and Jaenisch, R. (2005). Ectopic expression of Oct-4 blocks progenitor-cell differentiation and causes dysplasia in epithelial tissues. Cell *121*, 465–477.

Imhof, B.A., Vollmers, H.P., Goodman, S.L., and Birchmeier, W. (1983). Cell-cell interaction and polarity of epithelial cells: specific perturbation using a monoclonal antibody. Cell *35*, 667–675.

Kanatsu-Shinohara, M., Ogonuki, N., Inoue, K., Miki, H., Ogura, A., Toyokuni, S., and Shinohara, T. (2003). Long-term proliferation in culture and germline transmission of mouse male germline stem cells. Biol. Reprod. *69*, 612–616.

Kanatsu-Shinohara, M., Inoue, K., Lee, J., Yoshimoto, M., Ogonuki, N., Miki, H., Baba, S., Kato, T., Kazuki, Y., Toyokuni, S., et al. (2004). Generation of pluripotent stem cells from neonatal mouse testis. Cell *119*, 1001–1012.

Kanatsu-Shinohara, M., Lee, J., Inoue, K., Ogonuki, N., Miki, H., Toyokun, S., Ikawa, M., Nakamura, T., Gura, A., and Shinohara,

T. (2008). Pluripotency of a single spermatogonial stem cell in mice. Biol. Reprod. *78*, 681–687.

Ko, K., Tapia, N., Wu, G.M., Kim, J.B., Arauzo-Bravo, M.J., Sasse, P., Glaser, T., Ruau, D., Han, D.W., Greber, B., et al. (2009). Induction of pluripotency in adult unipotent germline stem cells. Cell Stem Cell *5*, 87–96.

Ko, K., Arauzo-Bravo, M.J., Kim, J., Stehling, M., and Scholer, H.R. (2010). Conversion of adult mouse unipotent germline stem cells into pluripotent stem cells. Nat. Protoc. *5*, 921–928.

Ko, K., Reinhardt, P., Tapia, N., Schneider, R.K., Arauzo-Bravo, M.J., Han, D.W., Greber, B., Kim, J., Kliesch, S., Zenke, M., et al. (2011). Brief report: evaluating the potential of putative pluripotent cells derived from human testis. Stem Cells *29*, 1304–1309.

Kossack, N., Meneses, J., Shefi, S., Nguyen, H.N., Chavez, S., Nicholas, C., Gromoll, J., Turek, P., and Pera, R.R. (2009). Isolation and characterization of pluripotent human spermatogonial stem cell-derived cells. J. Androl. *30*, 130.

Kubota, H., Avarbock, M.R., and Brinster, R.L. (2003). Spermatogonial stem cells share some, but not all, phenotypic and functional characteristics with other stem cells. Proc. Natl. Acad. Sci. USA *100*, 6487–6492.

Kubota, H., Avarbock, M.R., and Brinster, R.L. (2004). Growth factors essential for self-renewal and expansion of mouse spermatogonial stem cells. Proc. Natl. Acad. Sci. USA *101*, 16489–16494.

Labosky, P.A., Barlow, D.P., and Hogan, B.L. (1994). Mouse embryonic germ (EG) cell lines: transmission through the germline and differences in the methylation imprint of insulin-like growth factor 2 receptor (Igf2r) gene compared with embryonic stem (ES) cell lines. Development *120*, 3197–3204.

Li, R.H., Liang, J.L., Ni, S., Zhou, T., Qing, X.B., Li, H.P., He, W.Z., Chen, J.K., Li, F., Zhuang, Q.A., et al. (2010). A mesenchymal-to-epithelial transition initiates and is required for the nuclear reprogramming of mouse fibroblasts. Cell Stem Cell *7*, 51–63.

Li, X., Pei, D.Q., and Zheng, H. (2014). Transitions between epithelial and mesenchymal states during cell fate conversions. Protein Cell *5*, 580–591.

Liu, Y., Giannopoulou, E.G., Wen, D.C., Falciatori, I., Elemento, O., Allis, C.D., Rafii, S., and Seandel, M. (2016). Epigenetic profiles signify cell fate plasticity in unipotent spermatogonial stem and progenitor cells. Nat. Commun. *7*, 11275.

Matsui, Y., Zsebo, K., and Hogan, B.L. (1992). Derivation of pluripotential embryonic stem cells from murine primordial germ cells in culture. Cell *70*, 841–847.

Morimoto, H., Lee, J., Tanaka, T., Ishii, K., Toyokuni, S., Kanatsu-Shinohara, M., and Shinohara, T. (2012). In vitro transformation of mouse testis cells by oncogene transfection. Biol. Reprod. *86*, 148, 1–11.

Niedenberger, B.A., Busada, J.T., and Geyer, C.B. (2015). Marker expression reveals heterogeneity of spermatogonia in the neonatal mouse testis. Reproduction *149*, 329–338.

Ocana, O.H., and Nieto, M.A. (2010). Epithelial plasticity, stemness and pluripotency. Cell Res. *20*, 1086–1088.

Ozturk, S. (2015). Telomerase activity and telomere length in male germ cells. Biol. Reprod. *92*, 53.

Pech, M.F., Garbuzov, A., Hasegawa, K., Sukhwani, M., Zhang, R.X.J., Benayoun, B.A., Brockman, S.A., Lin, S.D., Brunet, A., Orwig, K.E., et al. (2015). High telomerase is a hallmark of undifferentiated spermatogonia and is required for maintenance of male germline stem cells. Genes Dev. *29*, 2420–2434.

Polo, J.M., Anderssen, E., Walsh, R.M., Schwarz, B.A., Nefzger, C.M., Lim, S.M., Borkent, M., Apostolou, E., Alaei, S., Cloutier, J., et al. (2012). A molecular roadmap of reprogramming somatic cells into iPS cells. Cell *151*, 1617–1632.

Resnick, J.L., Bixler, L.S., Cheng, L., and Donovan, P.J. (1992). Long-term proliferation of mouse primordial germ cells in culture. Nature *359*, 550–551.

Samavarchi-Tehrani, P., Golipour, A., David, L., Sung, H.K., Beyer, T.A., Datti, A., Woltjen, K., Nagy, A., and Wrana, J.L. (2010). Functional genomics reveals a BMP-driven mesenchymal-to-epithelial transition in the initiation of somatic cell reprogramming. Cell Stem Cell *7*, 64–77.

Seandel, M., James, D., Shmelkov, S.V., Falciatori, I., Kim, J., Chavala, S., Scherr, D.S., Zhang, F., Torres, R., Gale, N.W., et al. (2007). Generation of functional multipotent adult stem cells from GPR125(+) germline progenitors. Nature *449*, 346.

Shu, X.D., and Pei, D.Q. (2014). The function and regulation of mesenchymal-to-epithelial transition in somatic cell reprogramming. Curr. Opin. Genet. Dev. *28*, 32–37.

Tokuda, M., Kadokawa, Y., Kurahashi, H., and Marunouchi, T. (2007). CDH1 is a specific marker for undifferentiated spermatogonia in mouse testes. Biol. Reprod. *76*, 130–141.

Youn, H., Kim, S.H., Choi, K.A., and Kim, S. (2013). Characterization of Oct4-GFP spermatogonial stem cell line and its application in the reprogramming studies. J. Cell Biochem. *114*, 920–928.

Zeisberg, M., and Neilson, E.G. (2009). Biomarkers for epithelial-mesenchymal transitions. J. Clin. Invest. *119*, 1429–1437.

Zheng, Y., Thomas, A., Schmidt, C.M., and Dann, C.T. (2014). Quantitative detection of human spermatogonia for optimization of spermatogonial stem cell culture. Hum. Reprod. *29*, 2497–2511.

Stem Cell Reports, Volume *8*

Supplemental Information

Mesenchymal to Epithelial Transition Mediated by CDH1 Promotes Spontaneous Reprogramming of Male Germline Stem Cells to Pluripotency

Junhui An, Yu Zheng, and Christina Tenenhaus Dann

Supplementary data

Supplemental Experimental Procedures

Figure S1

A

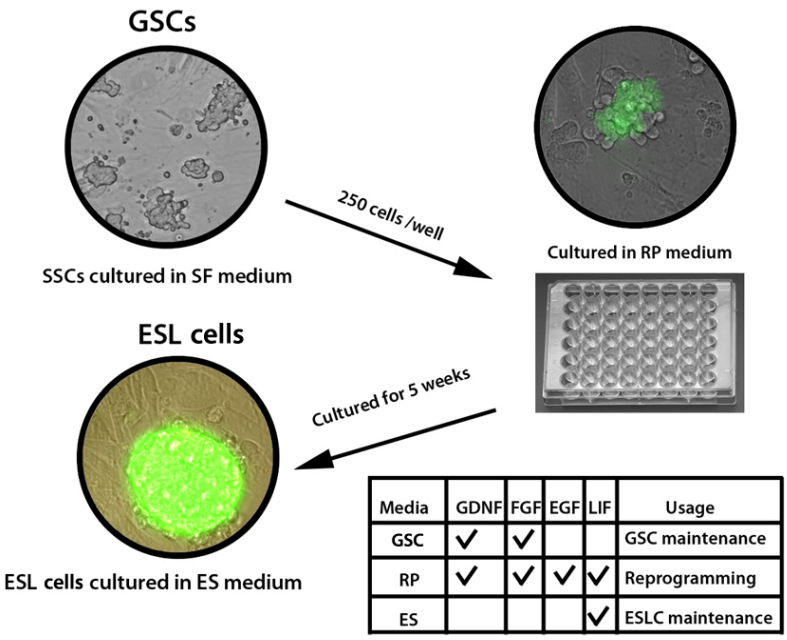

Media	GDNF	FGF	EGF	LIF	Usage
GSC	✓	✓			GSC maintenance
RP	✓	✓	✓	✓	Reprogramming
ES				✓	ESLC maintenance

B

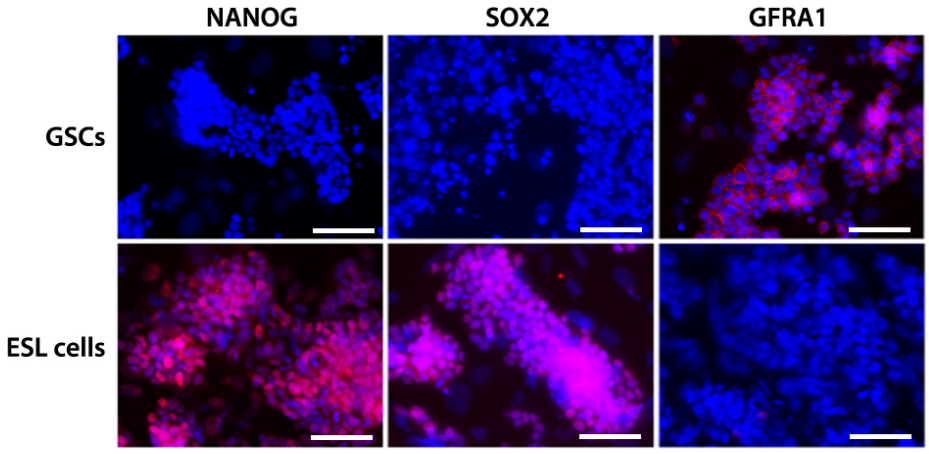

Figure S1. (Related to Figure 1) GSC reprogramming and ESL cell identification. (A) Schematic diagram of GSC reprogramming. Green color indicates Oct4-GFP expression. Image of ESL cells is intentionally equivalent to the data shown in Figure 1. (B) Immunofluorescence analysis of GSCs and ESL cells. Images of NANOG, SOX2 or GFRA1 immunostaining, shown in red, and DAPI (DNA) counterstaining, shown in blue, are merged. Bar=150 um.

Figure S2

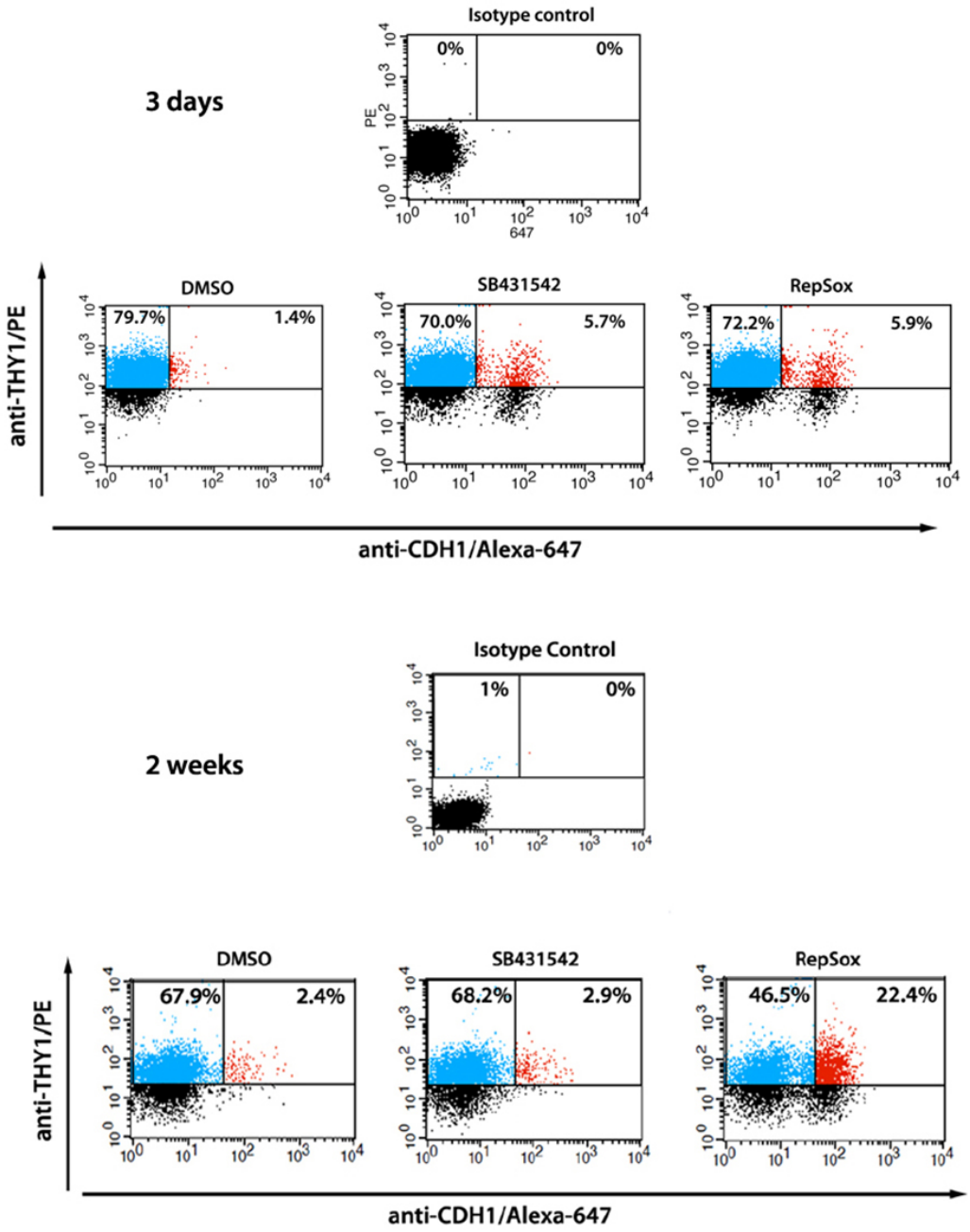

Figure S2. (Related to Figure 3) CDH1 and THY1 expression during reprogramming with TGFb inhibitor treatments. Dot plot showing CDH1 and THY1 expression in Oct4-GFP/Dox-Oct4 GSCs cultured in RP medium with DMSO (control), SB431542 (25μM) and RepSox (25μM) for 3 days (top) and 2 weeks (bottom). Trypsin was used for cell dissociation. Parent gates (not shown) include forward and side scatter to select singleton, viable cells. Percentages of the corresponding populations from GSCs are shown in parenthesis. Isotype controls were used to define background fluorescence for CDH1 and THY1 antibodies. The data shown are representative from three repeats of the same experiment.

Figure S3

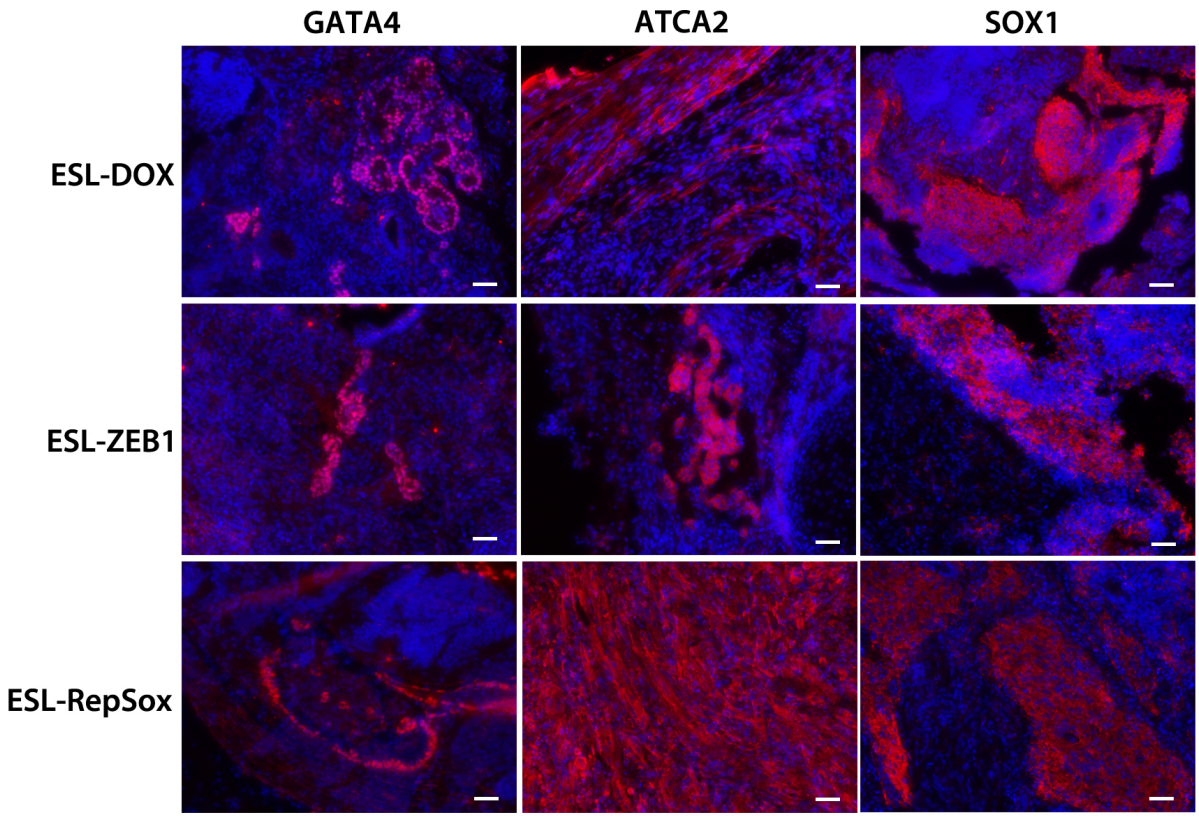

Figure S3. (Related to Figures 2, 3 and 4) Immunofluorescence analysis of teratomas derived from different ESL cells. ESL cells from doxycycline treated Dox-Oct4 GSCs (ESL-DOX), *Zeb1* siRNA treated GSCs (ESL-ZEB1) and RepSox treated GSCs were used for injections into NOD/SCID mice. GATA4, ACTA2 or SOX1 immunostaining, shown in red, and DAPI (DNA) counterstaining, shown in blue, are merged. Bar=150 um.

Figure S4

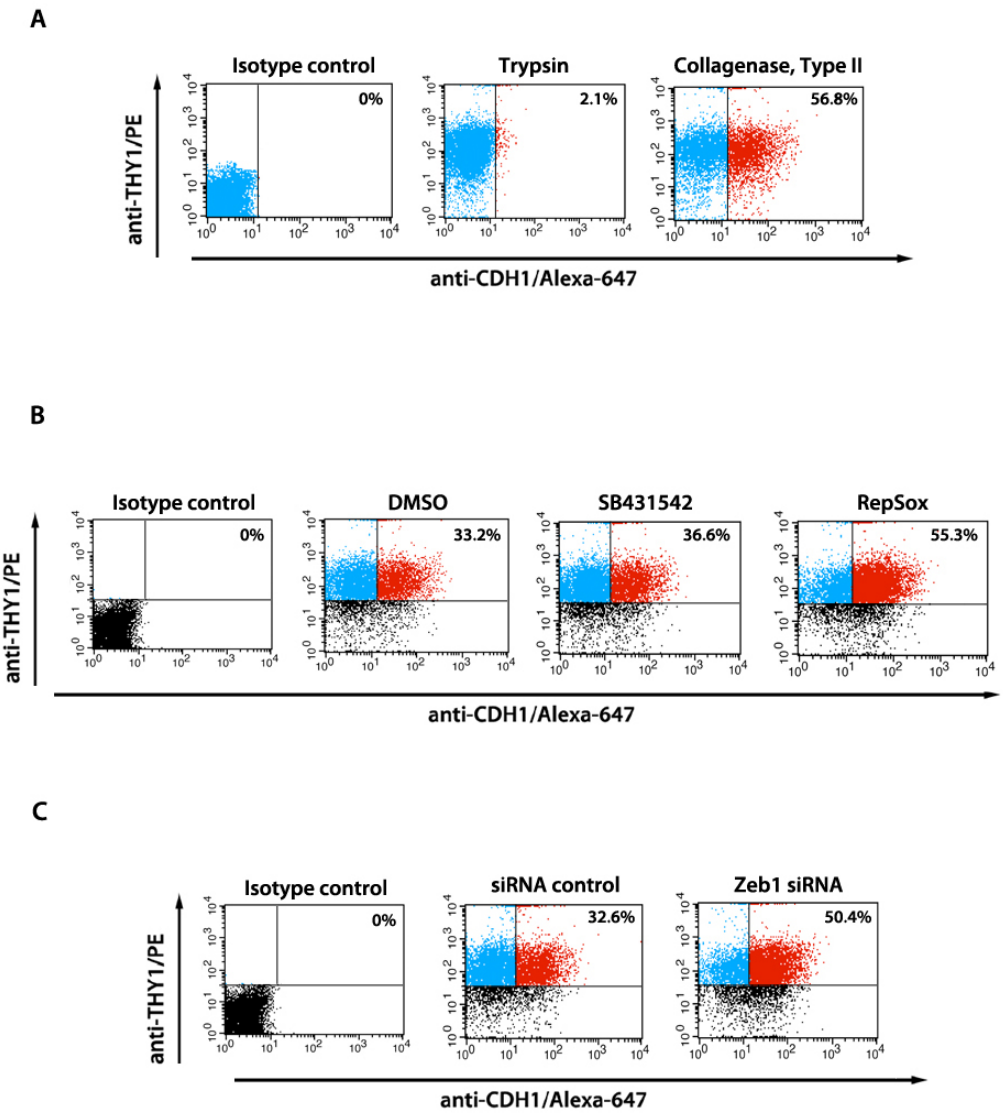

Figure S4. (Related to Figure 5) CDH1 and THY1 expression after collagenase type II digestion. (A) CDH1 and THY1 expression of Oct4-GFP/Dox-Oct4 GSCs after trypsin or collagenase, type II digestion. Dot plot showing CDH1 and THY1 expression in Oct4-GFP/Dox-Oct4 GSCs treated with TGF beta inhibitors (B, 25μM) and Zeb1 siRNA (C, 25nM) for 2 weeks. Collagenase type II was used for cell dissociation. Parent gates (not shown) include forward and side scatter to select singleton, viable cells. Percentages of the corresponding populations from GSCs are shown in parenthesis. Isotype controls were used to define background fluorescence for CDH1 and THY1 antibodies. The data shown are representative from three repeats of the same experiment.

Figure S5

A

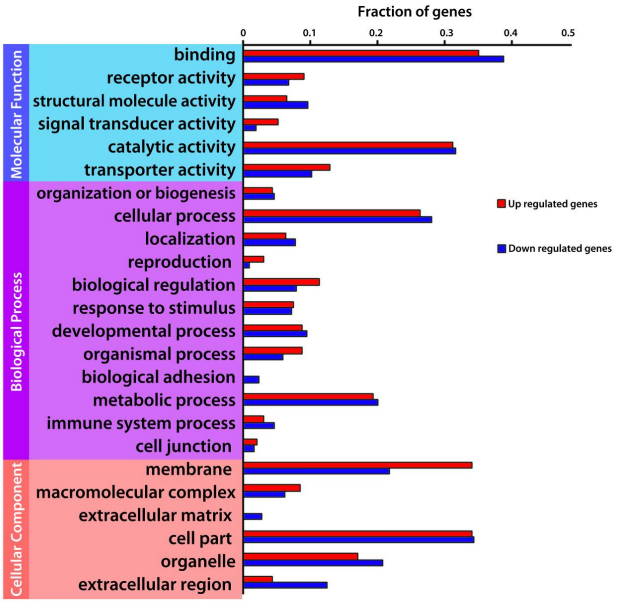

B

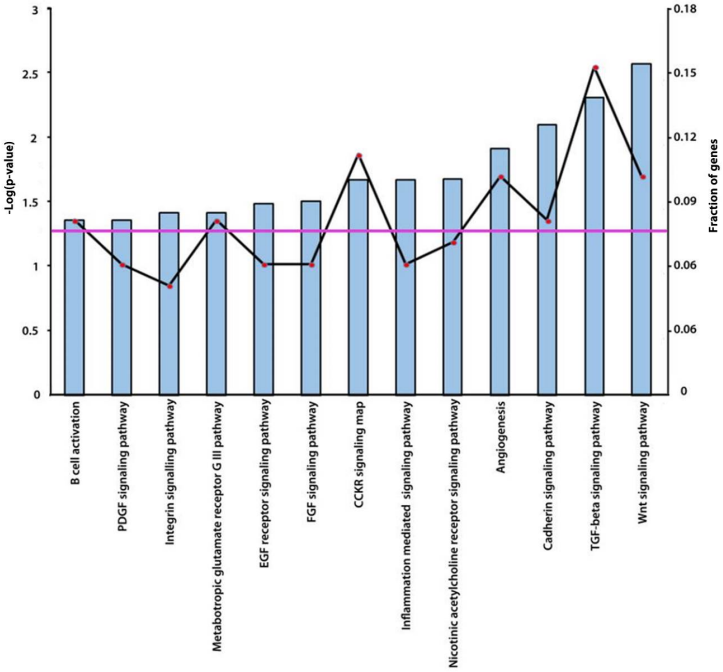

Figure S5. (Related to Figure 5) GO and signaling pathways analysis. (A) Gene Ontology (GO) enrichment analysis of differentially expressed genes ($Log_2FC>2$ or <-2) between CDH1+/THY1+ and CDH1-/THY1+ GSCs. Vertical axis displays the GO annotation corresponding to the three categories. Horizontal axis displays the fraction of significantly up regulated (red) or down regulated (blue) genes in each category. (B) Analysis of canonical signaling pathways in differentially expressed genes ($Log_2FC>2$ and <-2) between CDH1+/THY1+ and CDH1-/THY1+ GSCs. Major Y axis on the left shows the significance (-log (P-value)) of the canonical pathway (blue bar). Secondary Y axis on the right shows the percentage of differentially expressed genes involved in the canonical pathway (red point). The pink line shows the significance threshold cut off of -log (P-value = 0.05).

Figure S6

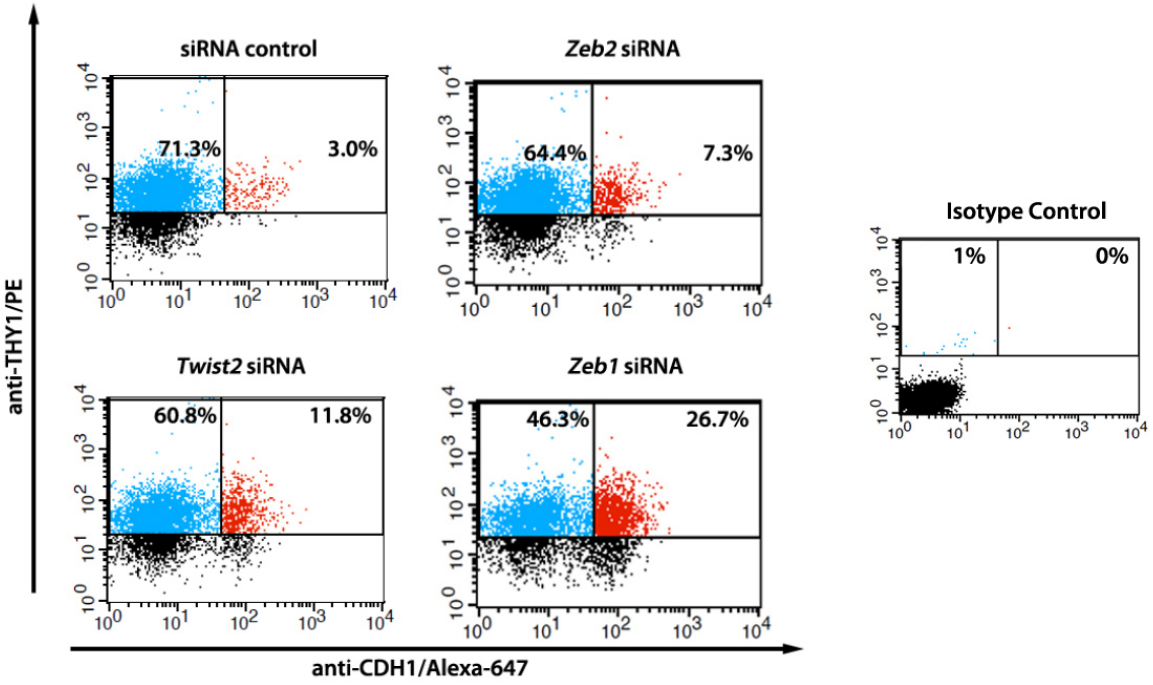

Figure S6. (Related to Figure 5) CDH1 and THY1 expression during reprogramming with knockdown of MET associated factors. Dot plot showing CDH1 and THY1 expression in Oct4-GFP/Dox-Oct4 GSCs cultured in RP medium with *Zeb1* siRNA, *Zeb2* siRNA, *Twist2* siRNA and siRNA control for two weeks. Trypsin was used for cell dissociation. Parent gates (not shown) include forward and side scatter to select singleton, viable cells. Percentages of the corresponding populations from GSCs are shown in parenthesis. Isotype controls were used to define background fluorescence for CDH1 and THY1 antibodies (not shown). The data shown are representative from three repeats of the same experiment.

Figure S7

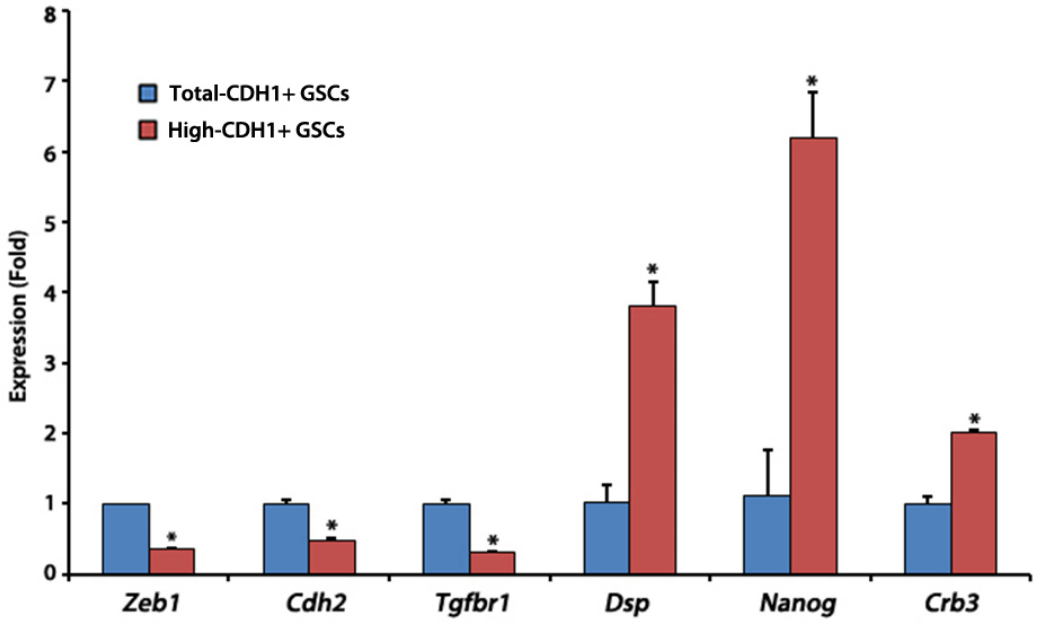

Figure S7. (Related to Figure 5) RT-QPCR analysis of indicated genes in high-CDH1+ cells and total-CDH1+ cells after collagenase type II digestion. High-CDH1+ Oct4-GFP/Dox-Oct4 GSCs (3% highest expressing CDH1 cells) and total-CDH1+ Oct4-GFP/Dox-Oct4 GSCs were sorted and used for RNA anlysis. Mean and SD for three biological replicates are shown. * p-value <0.01.

Table S1. (Related to Figure 1) Comparison of reprogramming media

	Shinahara (2004)	**Seandel (2007)**	**Ko (2009, 2010)**	**Guan (2009)**	**Takashima (2013)**
Base Meduim	**StemPro**	**StemPro**	**StemPro**	**#a-MEM**	**StemPro**
FBS	1%	1%	1%	1%	1%
Anti-biotic	1×	1×	1×	1×	1×
Insulin	25 μg/ml	25 μg/ml	5 μg/ml*	2 5 μg/ml*	25 μg/ml
transferrin	100 μg/ml	100 μg/ml	100 μg/ml*	100 μg/ml*	100 μg/ml
putrescine	60 μM	60 μM	100 μM*	60 μM*	60 μM
sodium selenite	30 nM	30 nM	30 nM*	30 nM*	30 nM
D-(+)-glucose	6 mg/ml	6 mg/ml	6 mg/ml	1 mg/ml#	6 mg/ml
pyruvic acid	30 μg/ml	30 μg/ml	30 mg/ml	n/a#	30 μg/ml
DL-lactic acid	1 μl/ml	11 μM	1 μl/ml	n/a#	1 μl/ml
bovine albumin	5 mg/ml	5 mg/ml	5 mg/ml	2.5 mg/ml#, *	5 mg/ml
l-glutamine	2 mM	2 mM	2 mM	2 mM#	2 mM
M 2-mercaptoethanol	50 μM	50 μM	50 μM (55 μM)	100 μM	50 μM
MEM vitamin solution	1×	1×	1×	1×	1×
NEAA	1×	1×	1×	1×	1×
ascorbic acid	100 μM	100 μM	n/a#	284 μM#	100 μM
d-biotin	10 μg/ml	10 μg/ml	n/a#	0.1 μg/ml#	10 μg/ml
β-estradiol	30 ng/ml	30 ng/ml	30 ng/ml		30 ng/ml
progesterone	60 ng/ml	60 ng/ml	6.3*+60 ng/ml	60 ng/ml*	60 ng/ml
EGF	20 ng/ml	20 ng/ml	20 ng/ml	n/a#	n/a#
FGF	10 ng/ml	10 ng/ml	10 ng/ml	n/a#	10 ng/ml
LIF	10^3 U/ml	10^3 U/ml	10^3 U/ml	10^3 U/ml	n/a#
GDNF	10 ng/ml	10 ng/ml	10 ng/ml *1× N2	4-20 ng/ml *1× N2-1	15 ng/ml
Mouse Age	0-2 days	3 weeks-8 months	5-8 weeks	2-5 weeks	0-2 days

*** an ingredient added as part of the N2 supplement; # notably different component**

Table S2. (Related to Figures 1-5) RT-qPCR and ChIP primers

Gene Name	Forward Primer (5' to 3')	Reserve Primer (5' to 3')
Cripto	ATGGACGCAACTGTGAACATGATGTTC GCA	CTTTGAGGTCCTGGTCCATCACGTGAC CAT
Utf1	GATGTCCCGGTGACTACGTCT	TCGGGGAGGATTCGAAGGTAT
Esg1	ATAAGCT TGATCTCGTCTTCC	CTTGCTAGGATGTAACAAA GC
Eras	TCAGATCCGCCTACTGCC	TTACCAACACCACTTGCACC
Zeb1	GCTGGCAAGACAACGTGAAAG	GCCTCAGGATAAATGACGGC
Zeb2	ATTGCACATCAGACTTTGAGGAA	ATAATGGCCGTGTCGCTTCG
Twist1	GGACAAGCTGAGCAAGATTCA	CGGAGAAGGCGTAGCTGAG
Twist2	CGCTACAGCAAGAAATCGAGC	GCTGAGCTTGTCAGAGGGG
Thy1	TGCTCTCAGTCTTGCAGGTG	TGGATGGAGTTATCCTTGGTGTT
Dsp	GGATTCTTCTAGGGAGACTCAGT	TCCACTCGTATTCCGTCTGGG
Cdh2	AGCGCAGTCTTACCGAAGG	TCGCTGCTTTCATACTGAACTTT
Pkp1	AACCACTCTCCGCTCAAGAC	CTTCTGCCGTTTGACGGTCAT
Crb3	CACCGGACCCTTTCACAAATA	CCCACTGCTATAAGGAGGACT
Cdh1	CAGGTCTCCTCATGGCTTTGC	CTTCCGAAAAGAAGGCTGTCC
Snai1	CACACGCTGCCTTGTGTCT	GGTCAGCAAAAGCACGGTT
Snai2	TGGTCAAGAAACATTTCAACGCC	GGTGAGGATCTCTGGTTTTGGTA
TgfbrI	TCTGCATTGCACTTATGCTGA	AAAGGGCGATCTAGTGATGGA
Smad7	GGCCGGATCTCAGGCATTC	TTGGGTATCTGGAGTAAGGAGG
Oct4	CCTGCAGAAGGAGCTAGAACAGT	TGTTCTTAAGGCTGAGCTGCAA
Nanog	TGGTCCCCACAGTTTGCCTAGTTC	CAGGTCTTCAGAGGAAGGGCGA
actinB	GGCTGTATTCCCCTCCATC	TGCCAGATCTTCTCCATGTC
	Primers for ChIP	
	Forward Primer (5' to 3')	**Reserve Primer (5' to 3')**
E-Box1&2	GACAGGGGTGGAGGAAGTTG	CTGATTGGCTGGGGACGC
E-Box3	CCCAGCCAATCAGCGGC	GGGAACTCAGTAGTGCGCC

Table S3 (Related to Figures 1-5) Antibodies and dilutions used

Antibody (clone)	Company & Catalog No.	Dilution*
Goat anti-GFRA1	R&D systems, AF560	IF: 1:400
Mouse anti-OCT4 (C10)	Santa Cruz, sc-5279	WB: 1:250
Mouse anti-TUB (DM1A)	Biogenex, MU121-5UC	WB: 1:5000
Rabbit anti-pSMAD3 (C25A9)	Cell Signaling Technology, 9520	WB: 1:1000
Rabbit anti-NANOG	Millipore, ABD88	IF:1:100; WB:1:1000
Goat anti-CDH1	R&D systems, AF748	WB:1:500
Mouse anti-beta3 TUB (TU-20)	Cell Signaling Technology, 4466	WB:1:1000
Mouse anti-SSEA1-Cy3 (MC-480)	Millipore, MAB4301C3	IF:1:200
Mouse anti-SOX2 (20G5)	Thermo scientific, MA1-014	IF:1:200; WB:1:1000
Mouse anti-ACTA2 (1A4)	Calbiochem, 113200	IF:1:200
Goat anti-SOX1	R&D systems, AF3369	IF:1:200
Goat anti-GATA4 (C-20)	Santa Cruz, sc-1237	IF:1:200
Rabbit anti ZEB1 (H-102)	Santa Cruz, sc-25388	WB: 1:250

*** WB=Western Blot; IF= Immunofluorescence**

Table S4. (Related to Figure 1) Media composition

Ingredient	Company	F12KB medium	GSC medium	RP medium	ES medium
DMEM/F12	SIGMA	Base	n/a	n/a	n/a
Knock-Out DMEM/F12	GIBCO	n/a	n/a	n/a	Base
Stem Pro-34	GIBCO	n/a	Base	Base	n/a
Stem Pro supp	GIBCO	n/a	1×	1×	n/a
MEM vitamin	GIBCO	n/a	1×	1×	n/a
NEAA	GIBCO	1×	1×	1×	1×
Antibiot/myc	GIBCO	1×	1×	1×	1×
L-glutamine	HYCLONE	1×	1×	1×	1×
estradiol	SIGMA	n/a	30 ng/ml	30 ng/ml	n/a
progesterone	SIGMA	n/a	60ng/ml	60ng/ml	n/a
FBS	HYCLONE	n/a	1%	1%	15%
transferrin	SIGMA	n/a	100 μg/ml	n/a	n/a
insulin	GIBCO	n/a	25 μg/ml	n/a	n/a
Rat GDNF	PEPROTECH	10 ng/ml	10 ng/ml	10 ng/ml	n/a
human FGF	PEPROTECH	10 ng/ml	10 ng/ml	10 ng/ml	n/a
mouse EGF	GOLDBIOTECH	n/a	n/a	20 ng/ml	n/a
ESGRO	MILLIPORE	n/a	n/a	10^3 Unit/ml	n/a
putrescine	SIGMA	n/a	60 μm	n/a	n/a
selenite	SIGMA	n/a	30 nM	n/a	n/a
pyruvic acid	SIGMA	n/a	30 μg/ml	30 μg/ml	n/a
lactic acid	SIGMA	n/a	0.06%	0.06%	n/a
BME	SIGMA	50 μM	50 μM	50 μM	100 μM
ascorbic acid	SIGMA	n/a	100 μM	n/a	n/a
D-biotin	SIGMA	n/a	10 μg/ml	n/a	n/a
D-glucose	SIGMA	n/a	6 mg/ml	6 mg/ml	n/a
BSA	CALBIOCHEM	2 mg/ml	5 mg/ml	5 mg/ml	n/a
KSR	GIBCO	1%	n/a	n/a	n/a
B27 supp	GIBCO	1×	n/a	n/a	n/a

Supplemental Experimental Procedures

GSC line derivation

GSC lines were derived and maintained following published procedures with minor modifications (Dann, 2013; Falciatori et al., 2008; Heim et al., 2012; Kanatsu-Shinohara et al., 2003). Testes were collected from 2 to 8 weeks old transgenic or wild type mice. Testicular cells were dissociated with a standard two-step enzymatic procedure using 1 mg/ml type IV collagenase (Sigma) and then 0.25% Trypsin (Hyclone). Dissociated cells were plated on gelatin coated wells in F12KB medium (Supplementary Table 4), a GSC growth formulation based on findings of Aoshima et al (Aoshima et al., 2013), to remove a portion of the somatic cells through differential adherence (Supplementary Methods). Non-adhering cells were collected and cultured in F12KB medium on a feeder layer of mitotically inactivated DR4 MEFs (ATCC) for approximately one week. Use of F12KB permitted the enrichment of SSCs by trituration prior to subsequent culturing on DR4 MEFs in Stem Pro based medium (GSC medium) containing 10 ng/mL GDNF and 10 ng/mL FGF2 and 19 other supplements as described (Supplementary Table 4) (Heim et al., 2012; Kanatsu-Shinohara et al., 2003). SSCs/spermatogonia cultured in this manner are referred to as "GSCs" (Kanatsu-Shinohara et al., 2003).

Cell culture and cell sorting

GSCs were cultured on DR4 MEFs. GSC medium (Supplementary Table 4) was used for GSCs maintenance. ES-D3 cells (ATCC, CRL-11632) and ESL cells were maintained in ES medium (Supplementary Table 4). To obtain sufficient cells for sorting, GSCs were expanded at standard plating density in GSC medium for two weeks prior to trysinization. GSCs were trypsinized and incubated for 25 min at 4°C in PBS with 2% FBS and Alexa 647 anti-mouse CDH1 antibody (147307, Biolegend), PE anti-mouse THY1 antibody (105307, Biolegend) or the appropriate isotype controls (Biolegend). Sorting was performed on an Aria II (BD Bioscience).

For SSC sorting, testes were collected from 5 to 8 weeks old mice. Testicular cells were dissociated with a standard two-step enzymatic procedure using 1 mg/ml type IV collagenase (Sigma) and then 0.25% Trypsin (Hyclone). Dissociated cells were incubated for 25 min at 4°C in PBS with 2% FBS and Alexa 647 anti-mouse CDH1 antibody (147307, Biolegend), PE anti-mouse THY1 antibody (105307, Biolegend) or the appropriate isotype controls (Biolegend). Sorting was performed on an Aria II and cells were directly sorted to the 48-well plate for reprogramming (BD Bioscience).

siRNA transfection and inhibitor treatment

siRNAs were transfected into GSCs with Lipofectamine 2000 (ThermoFisher) according to the manufacturer's protocol. siGENOME SMARTpool siRNAs were from Dharmacon for mouse *Zeb2* (D-059671), *Twist2* (D-044881) and *Cdh1* (D-041028); Stealth siRNA was from Invitrogen for targeting *Zeb1* (MSS210696). Scrambled non-targeting siRNA was used as a control (SIC001, Sigma). All siRNAs were used at a concentration of 25 nM. For reprogramming experiments, fresh RP medium was applied to cells six hours after transfection with siRNAs and transfections were repeated every 7 days during the reprogramming period (generally four weeks). For RNA or protein isolation cells were lysed 72 h after transfection. For CDH1 cell analysis transfection was conducted every 7 days for a total of 14 days prior to flow cytometry.

RepSox (508158, EMD Millipore) and SB431542 (616464, EMD Millipore) were dissolved in DMSO. RepSox and SB431542 were used at a concentration of 25 μM. GSCs undergoing inhibitor treatments had medium containing freshly diluted inhibitor refreshed every 3 days. Medium containing DMSO was used as a control.

Flow cytometry for cell analysis

GSCs at different reprogramming time points were used for flow cytometry analysis after trypsin digestion. Inhibitors or siRNAs treated GSCs were digested by trypsin (0.05%, SH30236, hyclone) or collagenase type II (1 mg/ml, 17101015, Gibco) and used for analysis. Collagenase type II was dissolved in F12/DMEM. Cells were incubated with trypsin for 10 min or with collagenase type II for 40 min at 37° before analysis. For the analysis, cells were incubated for 25 min at 4°C in PBS with 2% FBS and Alexa 647 anti-mouse CDH1 antibody (147307, Biolegend), PE anti-mouse THY1 antibody (105307, Biolegend) or the appropriate isotype controls (Biolegend).

Flow cytometry was performed on a Calibur (BD Bioscience). Data was analyzed by CellQuest Pro software (BD Bioscience).

Embryoid body formation and cell differentiation

For embryoid body formation ESL cells were cultivated as embryoid bodies (EBs) in hanging drops in differentiation medium (ES medium without LIF) as described for standard mouse ESC differentiation (Spelke et al., 2011). Briefly, 20 µl drops containing 300 ESL cells were pipetted onto the lid of a culture dish filled with PBS and incubated in hanging drops for 2 days. EBs were collected and cultured in non-tissue culture treated petri dishes for 5 days. For ectodermal, mesodermal and endodermal lineage detection, single EBs were transferred into each well of a gelatin coated 48-well plate for immunofluorescence analyses. For cardiac cell differentiation, EBs were seeded into a gelatin coated 48 well plate and cultured in differentiation medium with 1% DMSO for 10-20 days.

Neuronal lineage differentiation was performed as described (Gaspard et al., 2009). Briefly, ESL cells were cultured on gelatin-coated 60 mm dish for 12 days in DDM medium (DMEM/F12 supplemented with N2 supplement (1X, Gibco), non-essential amino acids (1X, Hyclone), Glutamine (1X, Gibco), 1 mM of sodium pyruvate, 500mg/ml of BSA, 0.1 mM of 2-mercaptoethanol, penicillin and streptomycin (1X Hyclone). Cells were subsequently differentiated in N2/B27 medium (1:1 of DDM and Neurobasal/B27 medium) for 10 days. Cells were fixed in 4% paraformaldehyde (EMS) prior to immunofluorescence analysis.

Teratoma formation

6- to 8-week-old NOD-SCID mice obtained from the *In Vivo* Therapeutics Core at the IU Simon Cancer Center (Indianapolis) were used for injections. ESL cells were cultured on DR4 MEFs in ES medium until they were approximately 60-80% confluent. ESL cells suspended in ES medium at 2 x 10^7 cells/ml and mixed with an equal volume of Matrigel (356237, corning). Each mouse was injected with 2 x 10^6 cells subcutaneously into the flank. Teratomas were observed after three to four weeks and recovered for analysis. Teratomas were fixed in formalin overnight at 4 °C and embedded in paraffin for sectioning and processed for immunohistochemical detection of germ layer markers.

Cell immunostaining and histological analysis (includes cell staining)

Cells in plates were fixed in 4% (v/v) paraformaldehyde for 15 min at room temperature and rinsed three times in TBS for 5 min before staining. For nuclear antibodies, cells were treated with TBS containing 0.1% tritonX-100 for 10 min. Cells were blocked for 2 hours in TBS containing 3% (w/v) bovine serum albumin (Jackson ImmunoResearch). Teratomas were embedded in paraffin and sections were washed in xylene and rehydrated through an ethanol series using standard techniques. Antigen retrieval was performed by boiling in Tris (10mM) /EDTA (1mM) antigen retrieval solution (pH=9.0) for 15 min. Primary antibodies and dilutions are listed in Supplementary Table 3. Primary antibodies were applied overnight at 4 °C. Appropriate secondary antibodies conjugated with Alexa-594 (Life Technologies), Alexa-488 (Life Technologies) or Cy3 (Jackson ImmunoResearch) were diluted (1:500) in TBS and applied for one hour at room temperature. For a negative control the primary antibody was omitted. Images were obtained using a Nikon Eclipse TiS inverted microscope equipped with a Retiga 2000R Fast 1394 camera. Images were acquired with Q-capture Pro software and Image J was used for pseudocoloring and to create overlays of colors.

RNA sequencing and transcriptome assembly

Two Oct4-GFP/Dox-Oct4 GCS lines (#1 and #2) and one wildtype GSC line (#3) were used for sorting CDH1-/THY1+ and CDH1+/THY1+ cells. RNAs were isolated using RNeasy-plus micro kit (74034, Qiagen). Libraries for each sample were constructed using the Illumina TruSeq Stranded Total RNA Library Prep Kit / Ribo-Zero Gold kit as per manufacturer's instructions. Libraries were quantified using an Agilent 2200 TapeStation, pooled equimolar and sequenced on an Illumina NextSeq500 instrument using a NextSeq150-v2 Mid Output reagent kit and flowcells. Scatter plot were generated by using core R functions (version 3.3.1). NextSeq read sequences were cleaned using Trimmomatic (version 0.32) to remove adapter sequences and perform quality trimming. The resulting paired reads were mapped against GRCm38.p4 using TopHat2 (version 2.1.1). Tophat uses Bowtie, which is based on the

Burrows-Wheeler transform algorithm, for sequence alignment and allows for mapping across exon junctions. Read counts for each gene were created using featureCount (version 1.5.0-p3) and Gencode m9 as the annotation. Custom Perl scripts were used for estimation of transcript abundances based on Fragments Per Kilobase of exon per Million fragments mapped (FPKM). Differential expression analysis was carried out using the DESeq2 package (version 1.12.3) in R/Bioconductor (R version 3.3.1). The combination of Blast2GO, WEGO, Kyoto Encyclopedia of Genes and Genomes (KEGG) and GO (Gene Ontology) database were used for further analysis. The data discussed in this publication have been deposited in NCBI's Gene Expression Omnibus (Edgar *et al*., 2002) and are accessible through GEO Series accession number GSE90712 (https://www.ncbi.nlm.nih.gov/geo/query/acc.cgi?acc=GSE90712).

RT-qPCR

RNA was isolated using the RNeasy plus micro kit (74034, Qiagen) according to the manufacturer's protocol. First-strand cDNA was produced using a qScript cDNA Synthesis Kit (23104, Quanta). For real-time PCR, a MX3000p Real-Time PCR system (Agilent) and Maxima SYBR Green/Rox qPCR Master Mix (ThermoFisher Scientific) were used according to the manufacturer's protocols. Transcript levels were normalized to b-Actin. qPCR conditions were 95°C for 10 min, 40 cycles at 95 °C for 15 s, 60 °C for 30 s, and 72 °C for 30 s, and then a melt curve analysis was performed to verify the quality of the amplicon. ΔΔCt method was used to calculate relative fold-changes, as described (Livak and Schmittgen, 2001). The PCR primers used in the experiments are shown in Supplementary Table 2.

Western Blotting

Cells were washed in PBS prior to lysis. Cells were trypsinized and resuspended in sample buffer ("SB", Laemmli buffer with 0.1M DTT) and boiled at 100 °C for 10 min. Lysates were electrophoresed through a 10% SDS-PAGE gel and transferred onto PVDF membrane using standard procedures. Following blocking in 5% milk with TBS, the membrane was incubated in primary antibody overnight at 4 °C. After washing, the membrane was incubated in IgG-HRP secondary antibody and washed. Supersignal West Femto (ThermoFisher Scientific) was used for detection. Blots were stripped using standard procedures and re-probed with anti-Tubulin (DM1A clone) to verify even loading.

Chromatin Immunoprecipitation (ChIP)

GSCs were transfected with *Zeb1* siRNA or control siRNA at 25 nM final concentration, using Lipofectamine 2000 (Invitrogen). After 3 days culture, ChIP was conducted according to the manufacturer's instructions by using EZ-ChIP Kit (Millipore). Briefly, cells (1×10^7) were cross-linked with 1% formaldehyde for 10 min at room temperature. Glycine was added to stop cross-linking, and cells were washed with cold PBS and harvested in SDS lysis buffer plus Protease Inhibitor Mixture II. Cell lysates were sonicated on ice by using a sonicator (Misonix S4000) for 8 cycles of 20 sec pulse at 40% power with 40 sec rest between each cycle. 1 % of each sample was used for gel analysis and confirmed to be sheared with DNA fragment sizes ranging from about 500 to 1000 bp. Immunoprecipitations were performed using 10 μg each of Anti-Zeb1 (Santa Cruz) or 10 ug Rabbit IgG overnight at 4 °C with rotation. Samples were mixed with Protein G Agarose and rotated at 4 °C for 1h. After washing, samples were eluted and purified. Maxima SYBR Green mix (Thermo Scientific) was used to perform real-time PCR on an MX3000p real-time PCR system (Agilent). The relative proportions of immunoprecipitated gene fragments were determined on the basis of the threshold cycle (Ct) for each PCR product. Data sets were normalized to ChIP input values. For every gene fragment analyzed, each sample was quantified in duplicate and from at least three independent ChIP experiments.

Reference

Aoshima, K., Baba, A., Makino, Y., and Okada, Y. (2013). Establishment of Alternative Culture Method for Spermatogonial Stem Cells Using Knockout Serum Replacement. Plos One *8*.
Dann, C.T. (2013). Transgenic modification of spermatogonial stem cells using lentiviral vectors. Methods in molecular biology (Clifton, NJ) *927*, 503-518.
Edgar R, Domrachev M, Lash AE (2002). Gene Expression Omnibus: NCBI gene expression and hybridization array data repository. Nucleic Acids Res. *30*, 207-10.
Falciatori, I., Lillard-Wetherell, K., Wu, Z., Hamra, F.K., and Garbers, D.L. (2008). Deriving mouse spermatogonial stem cell lines. Methods Mol Biol *450*, 181-192.
Gaspard, N., Bouschet, T., Herpoel, A., Naeije, G., van den Ameele, J., and Vanderhaeghen, P. (2009). Generation of cortical neurons from mouse embryonic stem cells. Nat Protoc *4*, 1454-1463.
Heim, C.N., Fanslow, D.A., and Dann, C.T. (2012). Development of Quantitative Microscopy-Based Assays for Evaluating Dynamics of Living Cultures of Mouse Spermatogonial Stem/Progenitor Cells. Biology of Reproduction *87*.
Kanatsu-Shinohara, M., Ogonuki, N., Inoue, K., Miki, H., Ogura, A., Toyokuni, S., and Shinohara, T. (2003). Long-term proliferation in culture and germline transmission of mouse male germline stem cells. Biol Reprod *69*, 612-616.
Livak, K.J., and Schmittgen, T.D. (2001). Analysis of relative gene expression data using real-time quantitative PCR and the 2(T)(-Delta Delta C) method. Methods *25*, 402-408.
Spelke, D.P., Ortmann, D., Khademhosseini, A., Ferreira, L., and Karp, J.M. (2011). Methods for embryoid body formation: the microwell approach. Methods Mol Biol *690*, 151-162.